

# Genetic analysis of praziquantel response in schistosome parasites implicates a Transient Receptor Potential channel

Winka Le Clec'h, Frédéric D Chevalier, Ana Carolina A Mattos, Amanda Strickland, Robbie Diaz, Marina Mcdew-White, Claudia M Rohr, Safari Kinung'hi, Fiona Allan, Bonnie L Webster, et al.

▶ **To cite this version:**

Winka Le Clec'h, Frédéric D Chevalier, Ana Carolina A Mattos, Amanda Strickland, Robbie Diaz, et al.. Genetic analysis of praziquantel response in schistosome parasites implicates a Transient Receptor Potential channel. Science Translational Medicine, 2021, 13 (625), pp.eabj9114. 10.1126/scitranslmed.abj9114 . hal-03428154

**HAL Id: hal-03428154**
**https://hal.science/hal-03428154**

Submitted on 15 Nov 2021

**HAL** is a multi-disciplinary open access archive for the deposit and dissemination of scientific research documents, whether they are published or not. The documents may come from teaching and research institutions in France or abroad, or from public or private research centers.

L'archive ouverte pluridisciplinaire **HAL**, est destinée au dépôt et à la diffusion de documents scientifiques de niveau recherche, publiés ou non, émanant des établissements d'enseignement et de recherche français ou étrangers, des laboratoires publics ou privés.

bioRxiv preprint doi: https://doi.org/10.1101/2021.06.09.447779; this version posted June 10, 2021. The copyright holder for this preprint (which was not certified by peer review) is the author/funder, who has granted bioRxiv a license to display the preprint in perpetuity. It is made available under aCC-BY-NC 4.0 International license.

# Genetic analysis of praziquantel resistance in schistosome parasites implicates a Transient Receptor Potential channel

Winka Le Clec'h[1*§], Frédéric D. Chevalier[1§], Ana Carolina A. Mattos[2], Amanda Strickland[1], Robbie Diaz[1], Marina McDew-White[1], Claudia M. Rohr[3], Safari Kinung'hi [4], Fiona Allan[5,6], Bonnie L Webster [5,6], Joanne P Webster [5,7], Aidan M Emery [5,6], David Rollinson [5,6], Amadou Garba Djirmay [8,9], Khalid M Al Mashikhi [10], Salem Al Yafae [10], Mohamed A Idris [11], Hélène Moné [12], Gabriel Mouahid [12], Philip LoVerde[2], Jonathan S. Marchant[3], Timothy J.C. Anderson[1*]

[1] Texas Biomedical Research Institute; San Antonio, TX

[2] University of Texas Health Science Center at San Antonio; San Antonio, TX 78229

[3]Department of Cell Biology, Neurobiology and Anatomy, Medical College of Wisconsin; Milwaukee WI 53226, USA.

[4] National Institute for Medical Research, Mwanza, United Republic of Tanzania

[5] London Centre for Neglected Tropical Disease Research (LCNDTR), Imperial College, London, United Kingdom

[6] Wolfson Wellcome Biomedical Laboratories, Natural History Museum, London, United Kingdom

[7] Centre for Emerging, Endemic and Exotic Diseases (CEEED), Royal Veterinary College, University of London, United Kingdom

[8] Réseau International Schistosomiases Environnemental Aménagement et Lutte (RISEAL), Niamey, Niger

[9] World Health Organization, Geneva, Switzerland

[10] Directorate General of Health Services, Dhofar Governorate, Salalah, Sultanate of Oman

[11] Sultan Qaboos University, Muscat, Sultanate of Oman

[12] Host-Pathogen-Environment Interactions laboratory, University of Perpignan, Perpignan, France

[§] These authors contributed equally to this work.

*Correspondence to: winkal@txbiomed.org (WL), tanderso@txbiomed.org (TA)

bioRxiv preprint doi: https://doi.org/10.1101/2021.06.09.447779; this version posted June 10, 2021. The copyright holder for this preprint (which was not certified by peer review) is the author/funder, who has granted bioRxiv a license to display the preprint in perpetuity. It is made available under aCC-BY-NC 4.0 International license.

27 **One Sentence Summary:** A transient receptor potential channel determines variation in praziquantel-

28 response in *Schistosoma mansoni*.

29

bioRxiv preprint doi: https://doi.org/10.1101/2021.06.09.447779; this version posted June 10, 2021. The copyright holder for this preprint (which was not certified by peer review) is the author/funder, who has granted bioRxiv a license to display the preprint in perpetuity. It is made available under aCC-BY-NC 4.0 International license.

**Abstract:**

Mass treatment with praziquantel (PZQ) monotherapy is the mainstay for schistosome treatment. This drug shows imperfect cure rates in the field and parasites showing reduced response to PZQ can be selected in the laboratory, but the extent of resistance in *Schistosoma mansoni* populations is unknown. We examined the genetic basis of variation in PZQ response in a *S. mansoni* population (SmLE-PZQ-R) selected with PZQ in the laboratory: 35% of these worms survive high dose (73 µg/mL) PZQ treatment. We used genome wide association to map loci underlying PZQ response. The major chr. 3 peak shows recessive inheritance and contains a transient receptor potential (*Sm.TRPM*$_{PZQ}$) channel (Smp_246790), activated by nanomoles of PZQ. Marker-assisted selection of parasites at a single *Sm.TRPM*$_{PZQ}$ SNP enriched populations of PZQ-R and PZQ-S parasites showing >377 fold difference in PZQ response. The PZQ-R parasites survived treatment in rodents better than PZQ-S. Resistant parasites show 2.25-fold lower expression of *Sm.TRPM*$_{PZQ}$ than sensitive parasites. Specific chemical blockers of *Sm.TRPM*$_{PZQ}$ enhanced PZQ resistance, while *Sm.TRPM*$_{PZQ}$ activators increased sensitivity. A single SNP in *Sm.TRPM*$_{PZQ}$ differentiated PZQ-ER and PZQ-ES lines, but mutagenesis showed this was not involved in PZQ-R, suggesting linked regulatory changes. We surveyed *Sm.TRPM*$_{PZQ}$ sequence variation in 259 individual parasites from the New and Old World revealing one nonsense mutation, that results in a truncated protein with no PZQ binding site. Our results demonstrate that *Sm.TRPM*$_{PZQ}$ underlies variation in PZQ response in *S. mansoni* and provides an approach for monitoring emerging PZQ-resistance alleles in schistosome elimination programs.

bioRxiv preprint doi: https://doi.org/10.1101/2021.06.09.447779; this version posted June 10, 2021. The copyright holder for this preprint (which was not certified by peer review) is the author/funder, who has granted bioRxiv a license to display the preprint in perpetuity. It is made available under aCC-BY-NC 4.0 International license.

## INTRODUCTION

Praziquantel (PZQ) is the drug of choice for treating schistosomiasis, a snail vectored parasitic disease, caused by flatworms in the genus *Schistosoma*. Schistosomiasis is widespread: three main parasite species infect over 140 million people in Africa, the Middle-East, South America and Asia *(1, 2)*, resulting in widespread morbidity – a global burden of 1.9 million disability adjusted life years *(3)* – and mortality estimates ranging from 20 to 280 thousand annually *(4, 5)*. Pathology results from eggs that lodge in the liver and intestine (*S. mansoni* and *S. japonicum*) or in the urogenital system (*S. haematobium*) stimulating granuloma formation. This results in a spectrum of pathology including portal hypertension, hepatosplenic disease, bladder cancer, genital schistosomiasis and infertility. *S. mansoni* infection alone results in a conservative estimate of 8.5 million cases of hepatosplenomegaly in sub-Saharan Africa *(6)*. Mass drug administration programs currently distribute an estimated 250 million doses of PZQ per year aimed in the short term at reducing schistosome associated morbidity and mortality, and in the longer term at eliminating schistosomiasis transmission *(7, 8)*. PZQ is also widely used for treatment of other flatworm parasites of both humans and livestock including tapeworms.

PZQ treatment of adult worms results in rapid $Ca^{2+}$ influx into cells, muscle contraction and tegument damage *(9–12)*. Both the mechanism of action and the mechanism of resistance to PZQ have been the focus for much speculation and research *(13, 14)*. Several proteins like calcium gated channels *(15–17)* or ABC transporters *(18, 19)* have been suspected to play a role in PZQ resistance. However, this topic has been stimulated by the recent finding that a transient receptor channel (*Sm.TRPM*$_{PZQ}$) is activated by nanomolar quantities of PZQ *(20, 21)*.

Mass drug treatment with PZQ has enormous health benefits and has been extremely effective in reducing parasite burdens and transmission *(8)*, but imposes strong selection for resistance on treated schistosome populations. Emergence of PZQ resistance is a major concern, because it could derail current progress towards WHO goal of eliminating schistosomiasis as a public health problem by 2025 *(8)*. Several lines of

bioRxiv preprint doi: https://doi.org/10.1101/2021.06.09.447779; this version posted June 10, 2021. The copyright holder for this preprint (which was not certified by peer review) is the author/funder, who has granted bioRxiv a license to display the preprint in perpetuity. It is made available under aCC-BY-NC 4.0 International license.

evidence from both the field and the laboratory suggest that PZQ response varies in schistosome populations *(22–27)*. PZQ resistance is readily selected in the laboratory through treatment of infected rodents or infected intermediate snail hosts *(28)*. This typically results in a modest change (3-5 fold) in PZQ response in parasite populations *(28, 29)*, although the PZQ resistance status of individual worms comprising these populations is unknown. PZQ treatment typically results in ~30% of patients who remain egg positive following PZQ treatment *(30)*. PZQ kills adult worms, but not immature parasites *(31, 32)*, so both newly emerging adult parasites and drug resistance may contribute to treatment failure. There have been several reports of patients who remained egg positive across multiple PZQ treatment cycles *(33, 34)*: schistosome infections established in mice from infective larvae from these patients showed elevated resistance to PZQ *(24, 35)*. In Kenya and Uganda, infected communities where prevalence and disease burden are not reduced by repeated treatment have been identified. The causes of these "hotspots" *(36, 37)* is currently unknown, but PZQ-resistant schistosomes are one explanation. In a large longitudinal study of individual school age children, egg reduction ratios (ERR) were high in naïve populations treated with PZQ, but showed a significant decline after multiple rounds of treatment *(38)*, consistent with selection of tolerance or resistance to PZQ. Identification of molecular markers for direct screening of levels of PZQ resistance alleles would be extremely valuable for parasite control programs, because changes in schistosome ERR have both genetic and non-genetic explanations and are laborious to measure.

The availability of good genome sequence and near complete genome assembly *(39)* for *S. mansoni* make unbiased genome wide approaches feasible for schistosome research *(40)*. Our central goal is to determine the genetic basis determinants of variation in PZQ response, using genome wide association approaches. We exploit the PZQ-resistant parasites generated by laboratory selection *(26)* to determine the genetic basis of PZQ, identifying a transient receptor channel as the cause of variation in PZQ response. The Transient Receptor Potential Melastatin (TRPM) ion channel identified is activated by PZQ *(20, 21)* and has been designated *Sm.TRPM*$_{PZQ}$. Together, our genetic analysis and the independent pharmacological analysis by

bioRxiv preprint doi: https://doi.org/10.1101/2021.06.09.447779; this version posted June 10, 2021. The copyright holder for this preprint (which was not certified by peer review) is the author/funder, who has granted bioRxiv a license to display the preprint in perpetuity. It is made available under aCC-BY-NC 4.0 International license.

97 Park *et al. (21)* identify the target channel for PZQ and provide a framework for monitoring PZQ resistance
98 evolution in schistosome control programs.

99 **RESULTS**

100 **PZQ resistant parasites are present in laboratory schistosome populations**

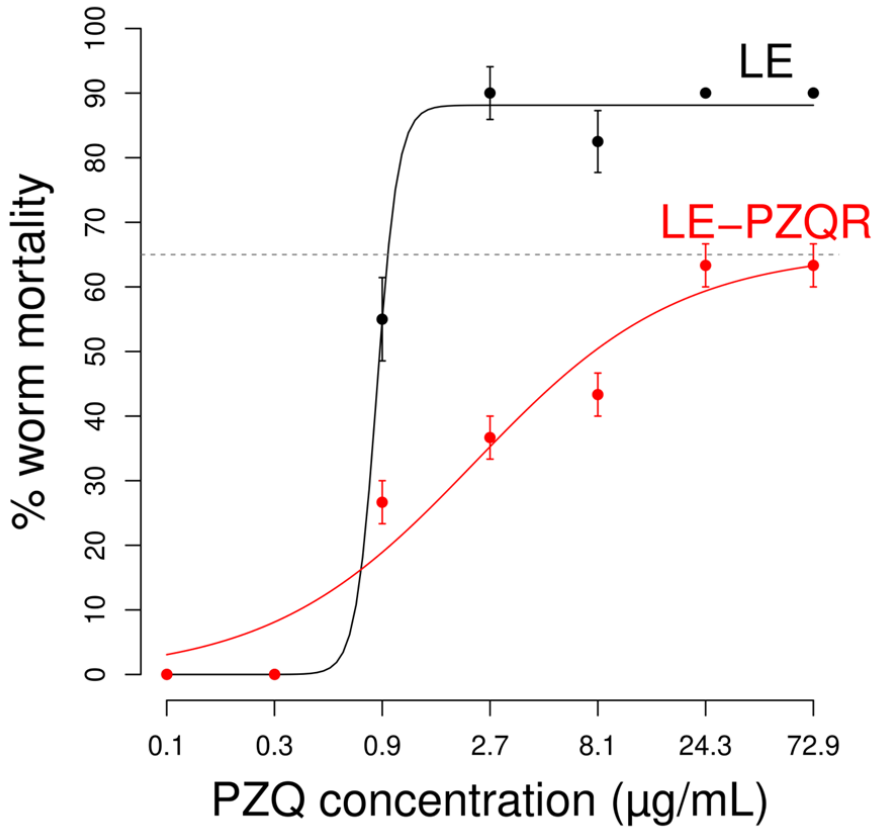



**Fig. 1. Dose response curves for SmLE (PZQ-S) and the derived SmLE-PZQ-R (PZQ-R) populations.** PZQ dose response curves show a ~14-fold difference in response between SmLE (ancestral population) and SmLE-PZQ (PZQ selected population) ($\chi^2$ test = 10.387, p = 0.001). The PZQ-selected laboratory schistosome population (LE-PZQ-R) is polymorphic for drug response. 35% of SmLE-PZQ-R are not killed by treatment with high dose of PZQ, suggesting that this population is polymorphic (*N*=240 worms/parasite populations).

bioRxiv preprint doi: https://doi.org/10.1101/2021.06.09.447779; this version posted June 10, 2021. The copyright holder for this preprint (which was not certified by peer review) is the author/funder, who has granted bioRxiv a license to display the preprint in perpetuity. It is made available under aCC-BY-NC 4.0 International license.

Male and female schistosome parasites pair in the blood vessels and reproduction is obligately sexual, so schistosomes are maintained in the laboratory as outbred populations. Hence, individual parasites within laboratory populations may vary in PZQ response. We measured PZQ response in the LE-PZQ-R population, which was previously generated by PZQ treatment of infected snails *(26)*. This revealed a 14-fold difference in $IC_{50}$ between the LE progenitor parasite population ($IC_{50}$=0.86 ± 0.14 µg/mL) and LE-PZQ-R ($IC_{50}$=12.75 ± 4.49 µg/mL, $\chi^2$ test, p = 0.001) derived by PZQ selection (Fig. 1). This is higher than the 3-5 fold differences observed between PZQ-selected and unselected parasite populations in previous studies *(28)*. Interestingly, the dose response curve for the LE-PZQ-R population plateaus at 65% mortality: the remaining 35% of parasites recovered even at high dose of PZQ (72.9 µg/mL). These results suggest that the LE-PZQ-R parasite population is a mixed population that contains both PZQ-sensitive and PZQ-resistant individual worms (Fig. 1).

**Association mapping of PZQ resistant genes identifies a TRPM channel**

We conducted a genome wide association study (GWAS) to determine the genetic basis of PZQ resistance (PZQ-R). GWAS has been widely used for mapping drug resistance in parasitic protozoa *(41)* and the model nematode *Caenorhabditis elegans (42)*, but has not previously been applied to parasitic helminths, because of the difficulty of accurately measuring drug response in individual parasites. When worms are treated with PZQ, there is a massive influx of $Ca^{2+}$ into cells and parasites contract *(17, 43)*, but some worms recover and resume respiration and movement 24-48h after drug removal. We assayed parasite recovery following high dose PZQ treatment (24 µg/mL) of individual male worms maintained in 96-well plates by measuring L-lactate production *(44)*, a surrogate measure of respiration, 48h after PZQ treatment removal (Fig. S1). These assays allow efficient measurement of recovery in individual PZQ-treated worms.

We conducted replicate experiments (A: n = 590; B: n = 691) to measure PZQ response in individual parasites maintained in 96-well plates. The distributions of L-lactate production in the two experiments

bioRxiv preprint doi: https://doi.org/10.1101/2021.06.09.447779; this version posted June 10, 2021. The copyright holder for this preprint (which was not certified by peer review) is the author/funder, who has granted bioRxiv a license to display the preprint in perpetuity. It is made available under aCC-BY-NC 4.0 International license.

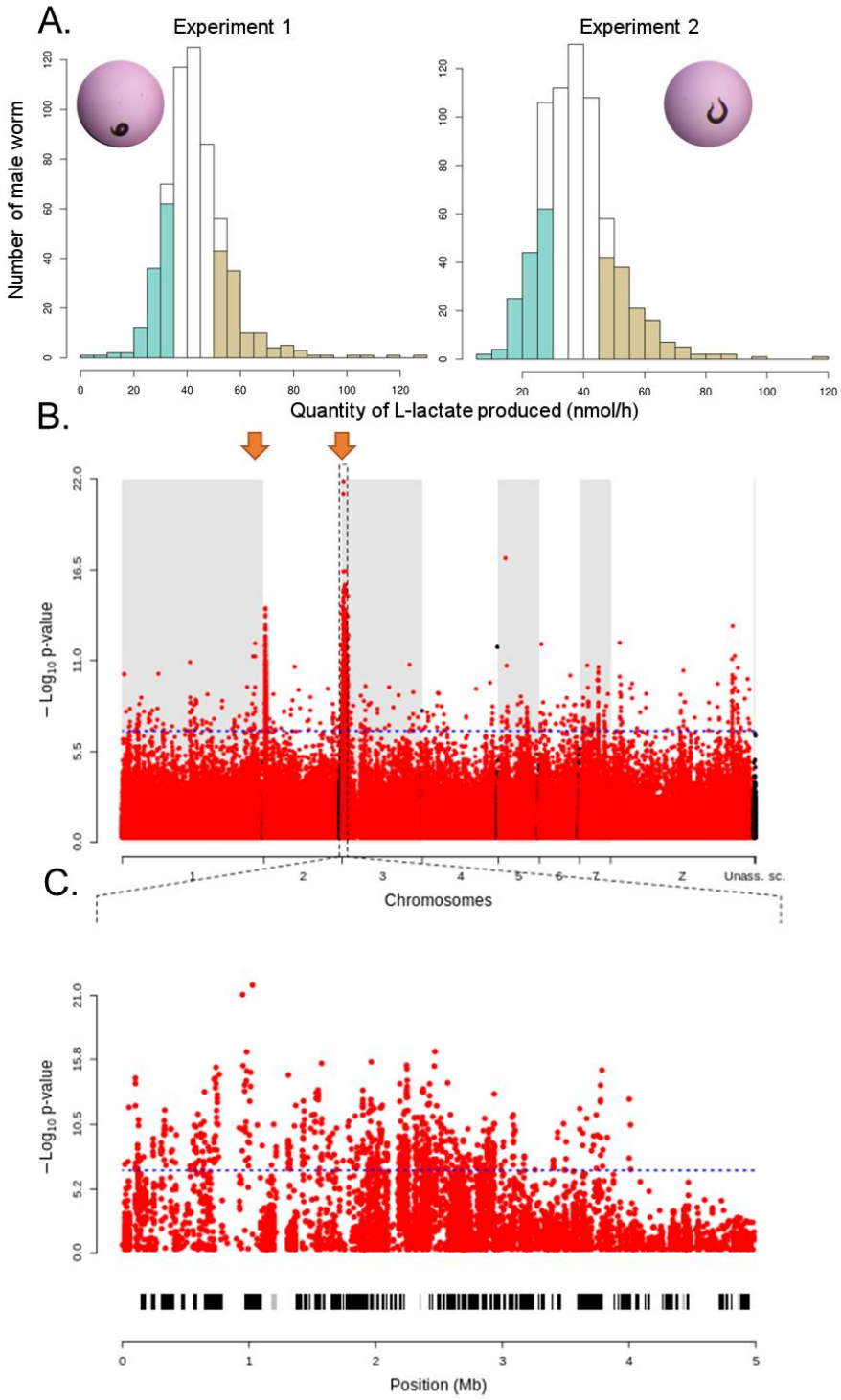



**Fig. 2. Genome-wide association mapping of PZQ response**. **(A).** We measured recovery of individual adult male worms following expose to 24µg/mL PZQ by measuring lactate production. The distribution from both experimental replicates is shown (A: *N*=590; B: *N*=691). Worms in the bottom and top quintile were each pooled, and genome sequenced to high read depth. **(B).** The Manhattan plot identifies genome regions that differ in allele frequency between high and low lactate worm pools. **(C).** The chr. 3 QTL identified spans 4 Mb and 91 genes, including several promising candidates.

bioRxiv preprint doi: https://doi.org/10.1101/2021.06.09.447779; this version posted June 10, 2021. The copyright holder for this preprint (which was not certified by peer review) is the author/funder, who has granted bioRxiv a license to display the preprint in perpetuity. It is made available under aCC-BY-NC 4.0 International license.

were broad (A: 0-126.56 nmol/h, mean = 42.95 nmol/h; B: 0-118.61 nmol/h, mean = 37.79 nmol/h): we identified worms from the top and bottom quintile for lactate production (Fig. 2A) which were then bulk sequenced to high read depth (average read depth - A: 39.97; B: 36.83). Two genome regions (chr. 2 and chr. 3) showed strong differentiation in allele frequencies between parasite populations showing high and low lactate production phenotypes (Fig. 2B). The highest peak ($p = 1.41 \times 10^{-22}$) on chr. 3 spanned 4 Mb (22,805-4,014,031 bp) and contained 91 genes, of which 85 are expressed in adult worms (Fig. 2C). This genome region contains several potential candidate loci including three partial ABC transporters (Table S1). One gene close to the highest association peak is of particular interest: Smp_246790 is a transient receptor potential channel in the M family (TRPM). This same channel was recently shown to be activated by PZQ following exposure to nM quantities of drug resulting in massive $Ca^{2+}$ influx into HEK293 cells transiently expressing this protein *(20, 21)*. This gene, designated *Sm.TRPM*$_{PZQ}$, is therefore a strong candidate to explain variation in PZQ response within parasite populations. Two other features of the data are of interest. First, the SNP (position 1029621 T>C) marking the highest association peak (at 1,030 Mb) is found in a transcription factor (Smp_345310, SOX13 homology) from a family known to regulate splicing variants *(45)*. Second, there is a ~100 kb deletion (1220683- 1220861 bp) 6.5 kb from *Sm.TRPM*$_{PZQ}$ and another 150 kb deletion (1,200,000-1,350,000 bp) 170 kb from the transcription factor. This was enriched in high lactate groups in both replicates and is in linkage disequilibrium with the enriched SNP in *Sm.TRPM*$_{PZQ}$.

The chr. 2 peak ($p < 1.0 \times 10^{-15}$) spans 1.166 Mb (291,191-1,457,462 bp) and contains 24 genes (21 expressed in adult worms). This genome region contains no genes that could be a candidate to explain variation in PZQ response.

bioRxiv preprint doi: https://doi.org/10.1101/2021.06.09.447779; this version posted June 10, 2021. The copyright holder for this preprint (which was not certified by peer review) is the author/funder, who has granted bioRxiv a license to display the preprint in perpetuity. It is made available under aCC-BY-NC 4.0 International license.

150 **PZQ resistance shows recessive inheritance**

151 To confirm these associations and determine whether the loci underlying PZQ response are inherited in a
152 dominant, co-dominant or recessive manner, we compared genotype and PZQ-response phenotype in
153 individual worms. We compared the L-lactate production phenotypes of individual worms maintained in
154 96-well plates 48 hours after exposure to 24 µg/mL PZQ with their genotypes at SNPs at the peaks of the
155 chr. 2 and chr. 3 QTLs. We also examined copy number of one of the 100 kb deletion observed on chr. 3
156 using qPCR. We observed significant differences in L-lactate production among genotypes (Fig. 3). Both

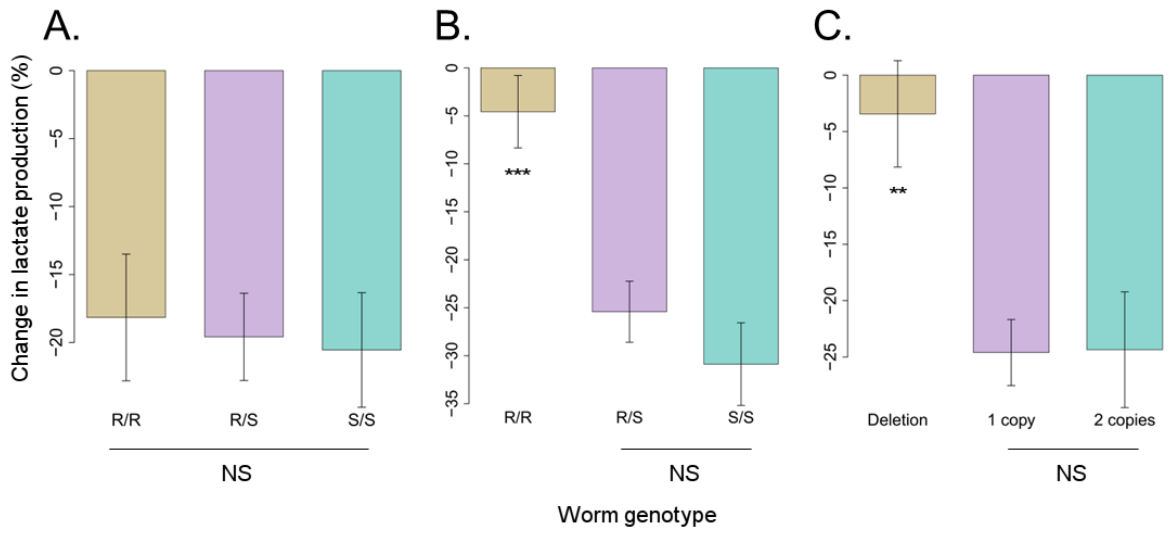



**Fig. 3. Inheritance of PZQ response in LE-PZQ population.** Bar charts show the change in L-lactate production after exposure to 24µg/mL PZQ in worms from different genotypic classes for QTL regions on chr. 2 and 3. **(A).** chr. 2 QTL (Kruskal-Wallis KW test $\chi^2 = 0.019$, p = 0.99), **(B).** *Sm.TRPM*$_{PZQ}$-741987C (KW test $\chi^2 = 24.481$, $p = 2.93 \times 10^{-6}$), **(C).** 100kb deletion (KW test $\chi^2 = 15.708$, p = 0.0004). We see minimal change in L-lactate production following PZQ exposure in homozygotes for the SNP enriched in PZQ treated parasites, indicating that this trait is recessive. Parasites carrying two copies of the 100 kb deletion are also strongly associated with resistance, demonstrating that this deletion is in LD ($N$ = 120 worms; NS: No significant difference between groups; *$p < 0.05$; ** $p \leq 0.01$; *** $p \leq 0.001$).

bioRxiv preprint doi: https://doi.org/10.1101/2021.06.09.447779; this version posted June 10, 2021. The copyright holder for this preprint (which was not certified by peer review) is the author/funder, who has granted bioRxiv a license to display the preprint in perpetuity. It is made available under aCC-BY-NC 4.0 International license.

the copy number variant and the SNP assayed in *Sm.TRPM*$_{PZQ}$ revealed that the causative gene in the chr. 3 QTL showed recessive inheritance. Homozygous parasites carrying two copies of the *Sm.TRPM*$_{PZQ}$-741987C allele (or two copies of the deletion) recovered from PZQ treatment, while the heterozygote and other homozygotes failed to recover from treatment (Fig. 3B-C). For the chr. 2 QTL, we did not see a significant association between parasite genotype and PZQ-R phenotype nor with lactate production before PZQ treatment (Fig. 3A): this locus was not investigated further.

## Marker-assisted purification of resistant and sensitive parasites

As the chr. 3 QTL containing *Sm.TRPM*$_{PZQ}$ shows the strongest association with PZQ response and shows recessive inheritance, we were able to use single generation marker assisted selection approach to enrich parasites for alleles conferring PZQ resistance (PZQ-R) and PZQ sensitivity (PZQ-S) from the mixed genotype LE-PZQ-R parasite population (Fig. 4A). We genotyped cercariae larvae emerging from snails previously exposed to single miracidia to identify parasites homozygous for the recessive PZQ-R allele from those homozygous for the PZQ-S allele. Parasites isolated from multiple snails falling into these two alternative genotypes were then used to infect hamsters. The enriched PZQ-resistant and sensitive parasites were designated SmLE-PZQ-ER and SmLE-PZQ-ES. Sequencing of adult parasites recovered from these two populations revealed that they were fixed for alternative alleles at the *Sm.TRPM*$_{PZQ}$-741987C SNP genotyped, but showed similar allele frequencies across the rest of the genome (Fig. S2). As expected, these sequences also revealed that the 100 kb deletion was close to fixation in the SmLE-PZQ-ER population (Fig. S3).

We conducted PZQ dose response curves on these enriched parasite populations. The SmLE-PZQ-ES population had an $IC_{50}$ of 0.193 µg/mL (± 1 s. d.: 0.045), while the SmLE-PZQ-ER population did not reach 50% reduction even at the highest dose (72.9 µg/mL) so has an $IC_{50}$ >72.9 µg/mL: the two purified populations differ by >377-fold in PZQ response (Fig. 4B). These results provide further demonstration

bioRxiv preprint doi: https://doi.org/10.1101/2021.06.09.447779; this version posted June 10, 2021. The copyright holder for this preprint (which was not certified by peer review) is the author/funder, who has granted bioRxiv a license to display the preprint in perpetuity. It is made available under aCC-BY-NC 4.0 International license.

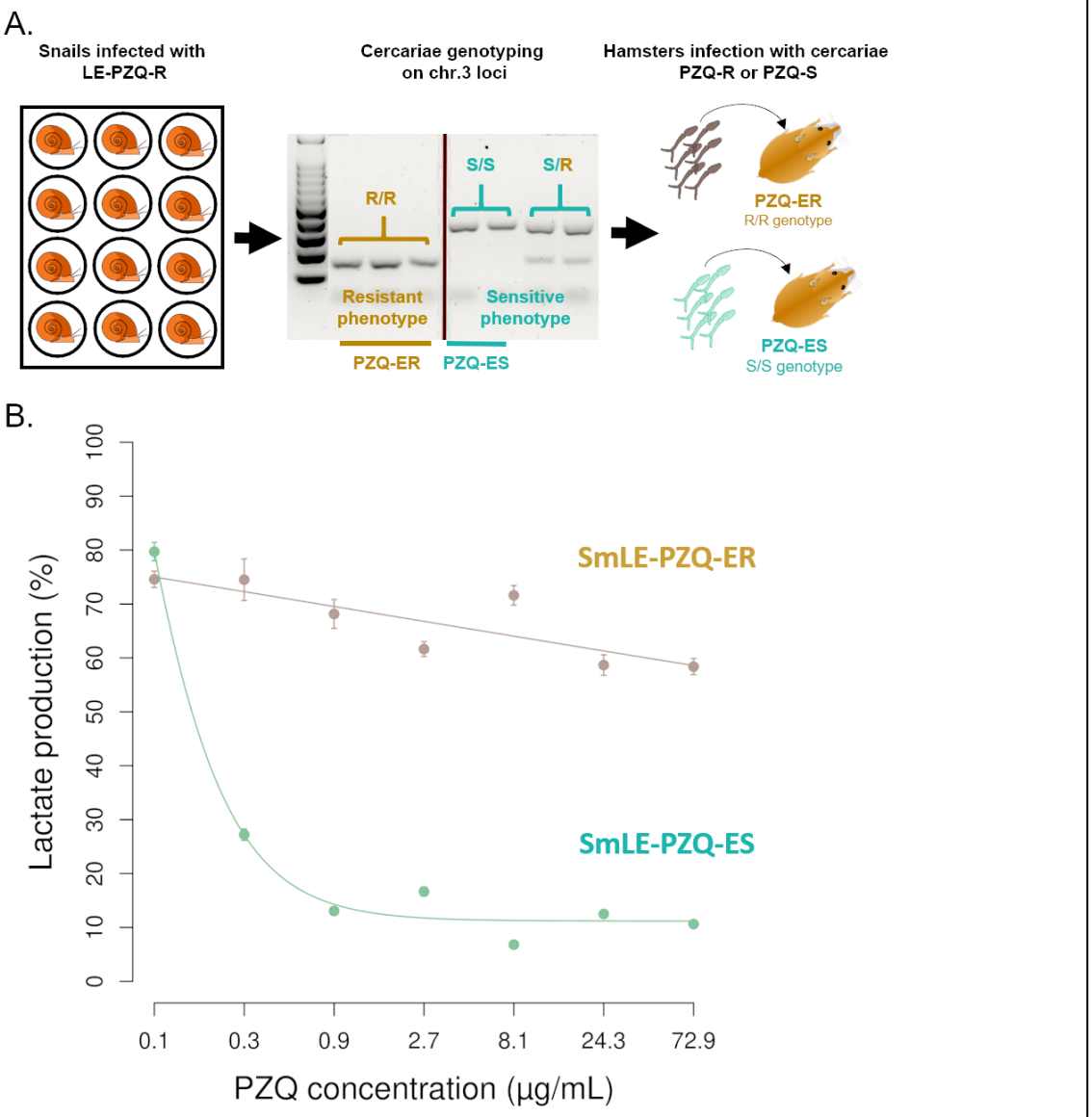



**Fig. 4. Single generation marker-assisted purification of SmLE-PZQ-ES and SmLE-PZQ-ER parasites.** **(A).** Experimental strategy for identifying parasite larvae that are homozygous for *Sm.TRPM*$_{PZQ}$ alleles associated with PZQ-R or PZQ-S. We genotyped cercaria larvae emerging from snails infected with single parasite genotypes for a restriction site in the *Sm.TRPM*$_{PZQ}$ gene, and then infected two groups of hamsters with parasites homozygous for alternative alleles at this locus. **(B).** The two populations of parasites generated show dramatic differences in PZQ-response ($N$ = 60 worms/population/treatment, $\chi^2$ test = 373.03, $p < 2.2 \times 10^{-16}$).

181

bioRxiv preprint doi: https://doi.org/10.1101/2021.06.09.447779; this version posted June 10, 2021. The copyright holder for this preprint (which was not certified by peer review) is the author/funder, who has granted bioRxiv a license to display the preprint in perpetuity. It is made available under aCC-BY-NC 4.0 International license.

that the original LE-PZQ-R parasite population was a mixture of PZQ-R and PZQ-S parasites. Separation of the component SmLE-PZQ-ES and SmLE-PZQ-ER parasites from these mixed populations allows rigorous characterization of the PZQ-R trait in parasite populations that are fixed for alternative alleles at *Sm.TRPM$_{PZQ}$*, but contain comparable genomic backgrounds across the rest of the genome.

### *Sm.TRPM$_{PZQ}$* gene and isoform expression is reduced in SmLE-PZQ-ER parasites

PZQ response varies between parasite stages and sexes, with strongest response in adult males. Adult females and juvenile worms are naturally resistant *(31, 32)*. We therefore examined gene expression in the purified SmLE-PZQ-ES and SmLE-PZQ-ER populations (males and females for both adults and juvenile worms) using RNA-seq (Fig. 5). Of the 85 genes expressed in adult worms under the chr. 3 QTL, only the *Sm.TRPM$_{PZQ}$* showed a significant reduction in expression in the SmLE-PZQ-ER adult male worms relative to SmLE-PZQ-ES (2.25-fold, posterior probability = 1) (Fig. 5A-B). Comparable under expression of *Sm.TRPM$_{PZQ}$* was also seen in female when compared to SmLE-PZQ-ES: expression of *Sm.TRPM$_{PZQ}$* was 11.94-fold lower in female than in male worms, consistent with females being naturally resistant *(31, 32)* (Fig. 5C). However, juvenile male and female worms showed elevated gene expression compared with adult worms (Fig. 5C). This is surprising because juveniles are naturally resistant to PZQ. *Sm.TRPM$_{PZQ}$* has 41 exons and occurs as 7 isoforms containing between 3 and 36 exons. Strikingly, SmLE-PZQ-ES male worms showed a 4.02-fold higher expression of isoform 6 compared to SmLE-PZQ-ER males, and an 8-fold higher expression than naturally resistant juvenile worms from both populations (while SmLE-PZQ-ER showed only a 2-fold higher expression) (Fig. 5B and D and Fig. S4). This suggests that high expression of isoform 6 is linked to PZQ sensitivity. The 15 exons of isoform 6 produce an 836 amino acid protein that lacks the transmembrane domain but contains the TRPM domain. We interrogated the 10x single cell expression data from adult worms *(46)* showing that *Sm.TRPM$_{PZQ}$* is expressed mainly in neural tissue with some expression also in muscle (Fig. S5).

bioRxiv preprint doi: https://doi.org/10.1101/2021.06.09.447779; this version posted June 10, 2021. The copyright holder for this preprint (which was not certified by peer review) is the author/funder, who has granted bioRxiv a license to display the preprint in perpetuity. It is made available under aCC-BY-NC 4.0 International license.

206

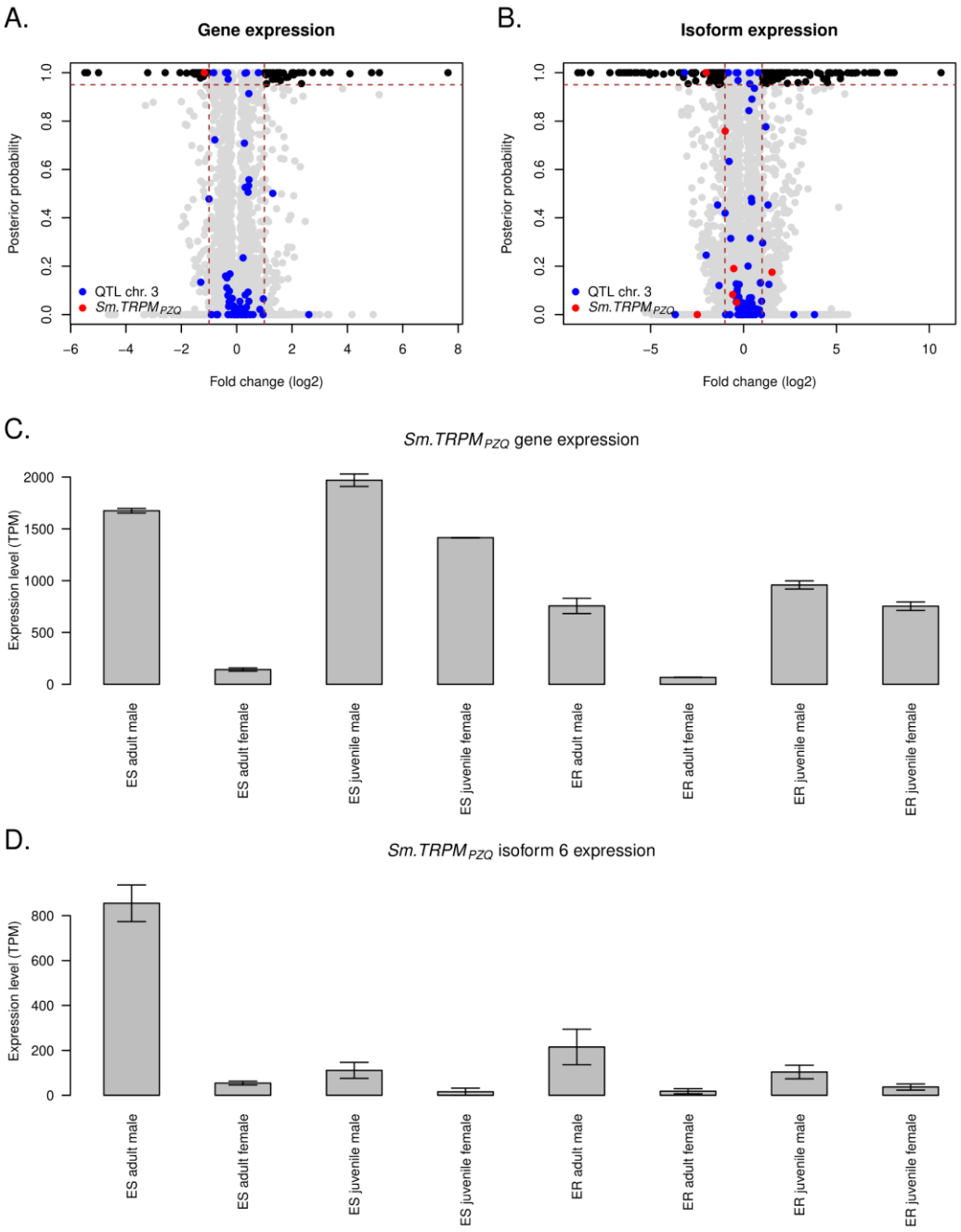



**Fig. 5. Gene expression differences between SmLE-PZQ-ES and SmLE-PZQ-ER parasites.** Volcano plot showing the differential **(A).** gene expression and **(B).** isoform expression between adult male PZQ-ES and PZQ-ER (In blue: genes located under the chr. 3 QTL, in red: *Sm.TRPM*$_{PZQ}$ gene). **(C).** *Sm.TRPM*$_{PZQ}$ gene expression and **(D).** *Sm.TRPM*$_{PZQ}$ isoform 6 expression level comparison between PZQ-ES and ER for the two sex (i.e. male and females) and different stages (i.e. adult and juvenile). High expression of *Sm.TRPM*$_{PZQ}$ isoform 6 is linked to PZQ sensitivity.

bioRxiv preprint doi: https://doi.org/10.1101/2021.06.09.447779; this version posted June 10, 2021. The copyright holder for this preprint (which was not certified by peer review) is the author/funder, who has granted bioRxiv a license to display the preprint in perpetuity. It is made available under aCC-BY-NC 4.0 International license.

## Fitness of SmLE-PZQ-ER and SmLE-PZQ-ES parasite populations

Both laboratory selected and field isolated *S. mansoni* showing PZQ-R have been difficult to maintain in the laboratory *(47)*: the PZQ-R trait has been rapidly lost consistent with strong selection against this trait. It has been suggested that PZQ-R carries a fitness cost that will slow spread of this trait in the field under PZQ pressure. Such fitness costs are a common, but not ubiquitous, feature of drug resistance in other pathogens *(48–50)*. We measured several components of parasite fitness in SmLE-PZQ-ES and SmLE-PZQ-ER parasites during laboratory passage of purified parasite lines, but found no significant differences in infectivity to snails, snail survival, or infectivity to hamsters (Fig. 6A). We did not see loss of PZQ-R in our lines after 12 generations because the key genome region is fixed. Cioli *et al. (28)* has also reported

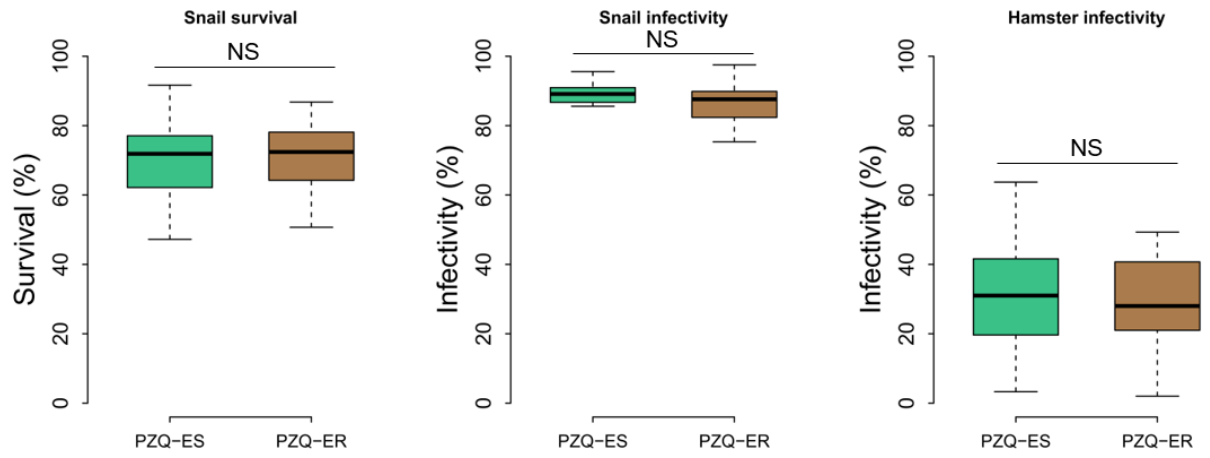



**Fig 6. Fitness of SmLE-PZQ-ES and SmLE-PZQ-ER parasites.** Comparison of several life history traits: Snail survival (Welsh t-test, t = -0.662, p = 0.51), infectivity to snails (Wilcoxon test, W = 123, p = 0.45), and infectivity to hamsters (Welsh t-test, t = 0.725, p = 0.47) for 12 generations of SmLE-PZQ-ER and SmLE-PZQ-ES parasites. (NS: No significant difference between groups).

bioRxiv preprint doi: https://doi.org/10.1101/2021.06.09.447779; this version posted June 10, 2021. The copyright holder for this preprint (which was not certified by peer review) is the author/funder, who has granted bioRxiv a license to display the preprint in perpetuity. It is made available under aCC-BY-NC 4.0 International license.

long term stability of PZQ-R parasite populations indicative that PZQ-R associated fitness costs maybe limited or absent.

### *In vivo* efficacy of PZQ against SmLE-PZQ-ES and SmLE-PZQ-ER parasites

To determine the relationship between *in vitro* PZQ-R measured in 96-well plates, and *in vivo* resistance, we treated mice infected with either SmLE-PZQ-ER or SmLE-PZQ-ES parasites populations with 120 mg/kg of PZQ. We observed no significant reduction in worm burden in SmLE-PZQ-ER parasites when comparing PZQ-treated and control (DMSO) treated animals (Wilcoxon test, p = 0.393; Fig. S6A). In contrast, we recovered significantly lower numbers of worms from PZQ-treated versus untreated mice infected with the SmLE-PZQ-ES parasite population (Wilcoxon test, p = 0.008; Fig. S6A). The percent reduction observed was significantly different between the SmLE-PZQ-ES and SmLE-PZQ-ER parasites (Wilcoxon test, p = 0.0129; Fig. S6B). Interestingly, we observed a large reduction in numbers of female worms recovered from PZQ-treated SmLE-PZQ-ES parasites relative to untreated animals (Wilcoxon test, p = 0.008; Fig. S6D), while for male worms this did not reach significance (Wilcoxon test, p = 0.089, Fig. S6C). We saw no impact of PZQ-treatment for either female or male worms in mice infected with SmLE-PZQ-ER. These results show that *in vivo* PZQ response in treated mice differs between SmLE-PZQ-ES and SmLE-PZQ-ER parasites. These data also suggest that the extended paralysis of male SmLE-PZQ-ES worms under PZQ treatment may reduce their ability to maintain female worms *in copula*.

### Chemical blockers and activators of *Sm.TRPM$_{PZQ}$* modulate PZQ-R

*Sm.TRPM$_{PZQ}$* emerges as a strong candidate gene to explain variation in PZQ response, but validation is required. We were unsuccessful in knocking down expression of *Sm.TRPM$_{PZQ}$* using either siRNA or dsRNA (Table S2), possibly because this gene is expressed mainly in neural tissue. We therefore used two

bioRxiv preprint doi: https://doi.org/10.1101/2021.06.09.447779; this version posted June 10, 2021. The copyright holder for this preprint (which was not certified by peer review) is the author/funder, who has granted bioRxiv a license to display the preprint in perpetuity. It is made available under aCC-BY-NC 4.0 International license.

chemical modulators of Sm.TRPM$_{PZQ}$ activity – an *Sm.TRPM$_{PZQ}$* agonist (AG1) and Sm.TRPM$_{PZQ}$ antagonist (ANT1). These were identified from a screen of ~16,000 compounds by screening $Ca^{2+}$ influx into HEK293 cells transiently expressing Sm.TRPM$_{PZQ}$ (Chulkov *et al.*, in prep). Addition of the Sm.TRPM$_{PZQ}$ blocker (antagonist ANT1) allowed SmLE-PZQ-ES worms to recover from PZQ treatment (Fig. 7A), while the Sm.TRPM$_{PZQ}$ activator (agonist AG1) rendered SmLE-PZQ-ER worms sensitive to PZQ treatment in a dose dependent manner (Fig. 7B). These results are consistent with a role for Sm.TRPM$_{PZQ}$ in determining variation in PZQ response.

We found 5 non-synonymous SNPs and 5 insertions that showed significant differences in allele frequency in *Sm.TRPM$_{PZQ}$* in the SmLE-PZQ-ES and SmLE-PZQ-ER parasite populations. One of these SNPs (*Sm.TRPM$_{PZQ}$*-741903) and two insertions (*Sm.TRPM$_{PZQ}$*-779355 and *Sm.TRPM$_{PZQ}$*-779359) are fixed for alternative alleles in the two populations, with 7 others are segregating at different frequencies in the two populations (Fig. S3). These SNPs are located outside the critical transmembrane domains so were not strong candidates to explain differences in PZQ-R. We expressed *Sm.TRPM$_{PZQ}$* carrying some of these variants in HEK293 cells and examined their impact on $Ca^{2+}$ influx to interrogate their role in explaining

bioRxiv preprint doi: https://doi.org/10.1101/2021.06.09.447779; this version posted June 10, 2021. The copyright holder for this preprint (which was not certified by peer review) is the author/funder, who has granted bioRxiv a license to display the preprint in perpetuity. It is made available under aCC-BY-NC 4.0 International license.

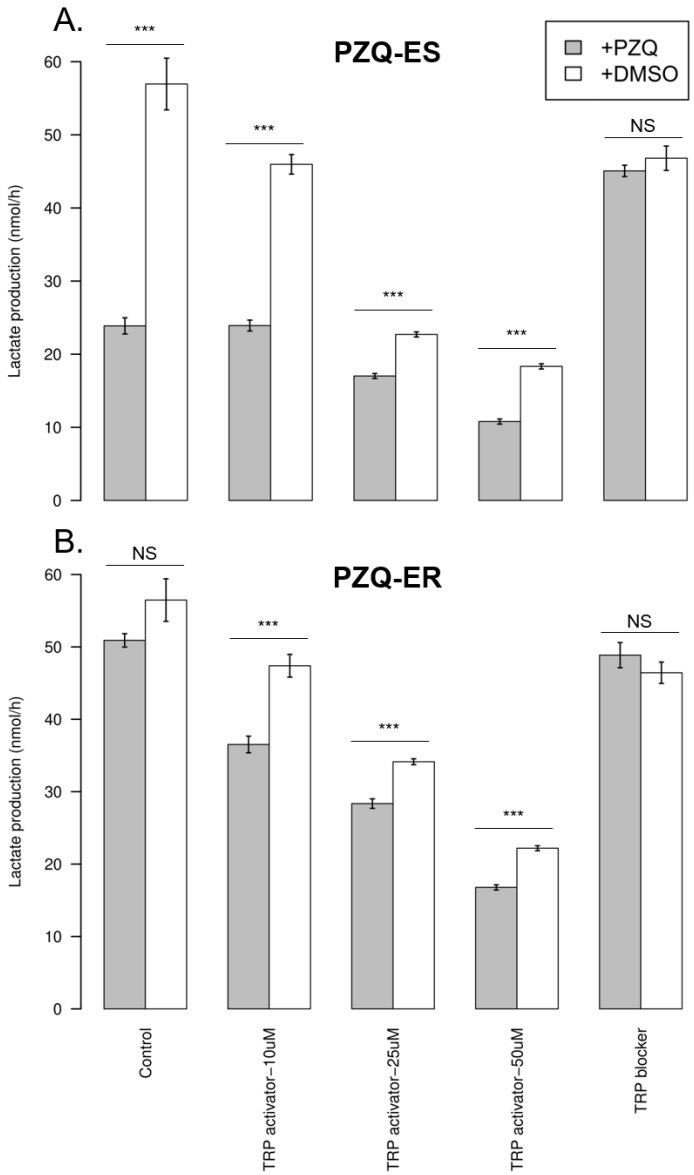



**Fig. 7. Impact of *Sm.TRPM$_{PZQ}$* blockers and activators on PZQ response.** (A) SmLE-PZQ-ES and (B) SmLE-PZQ-ER were exposed to either i) PZQ or DMSO alone (control group), ii) PZQ or DMSO combined with either 10 µM, 25 µM or 50 µM of Sm.TRPM$_{PZQ}$ activator (agonist AG1), iii) PZQ or DMSO combined with 50 µM Sm.TRPM$_{PZQ}$ blocker (antagonist ANT1). Parasite viability was assessed 3 days post-treatment, based on their L-lactate production). Addition of the Sm.TRPM$_{PZQ}$ blocker allowed SmLE-PZQ-ES worms to recover from PZQ treatment (Welsh t-test, t = -0.94, p = 0.35), while the Sm.TRPM$_{PZQ}$ activator (agonist AG1) rendered SmLE-PZQ-ER worms sensitive to PZQ treatment in a dose dependent manner (N = 20 worms/population/treatment; Welsh t-test, NS: No significant difference between groups; *$p < 0.05$; ** $p \leq 0.01$; *** $p \leq 0.001$.)

bioRxiv preprint doi: https://doi.org/10.1101/2021.06.09.447779; this version posted June 10, 2021. The copyright holder for this preprint (which was not certified by peer review) is the author/funder, who has granted bioRxiv a license to display the preprint in perpetuity. It is made available under aCC-BY-NC 4.0 International license.

underlie PZQ response. We speculate that the difference in PZQ response is due to expression patterns and may be controlled by regulatory variants potentially associated with the adjacent 100 kb deletion or the SOX13 transcription factor.

## Sequence variation in *Sm.TRPM$_{PZQ}$* from natural *S. mansoni* populations

Methods for evaluating frequencies of PZQ-resistance mutations in endemic regions would provide a valuable tool for monitoring mass treatment programs aimed at schistosome elimination. Both this paper and the accompanying paper *(21)* identify *Sm.TRPM$_{PZQ}$* as being critical to PZQ-response, and Park *et al*. have determined critical residues that determine binding between PZQ and *Sm.TRPM$_{PZQ}$ (21)*. We examined the mutations present in *Sm.TRPM$_{PZQ}$* in natural schistosome populations using exome

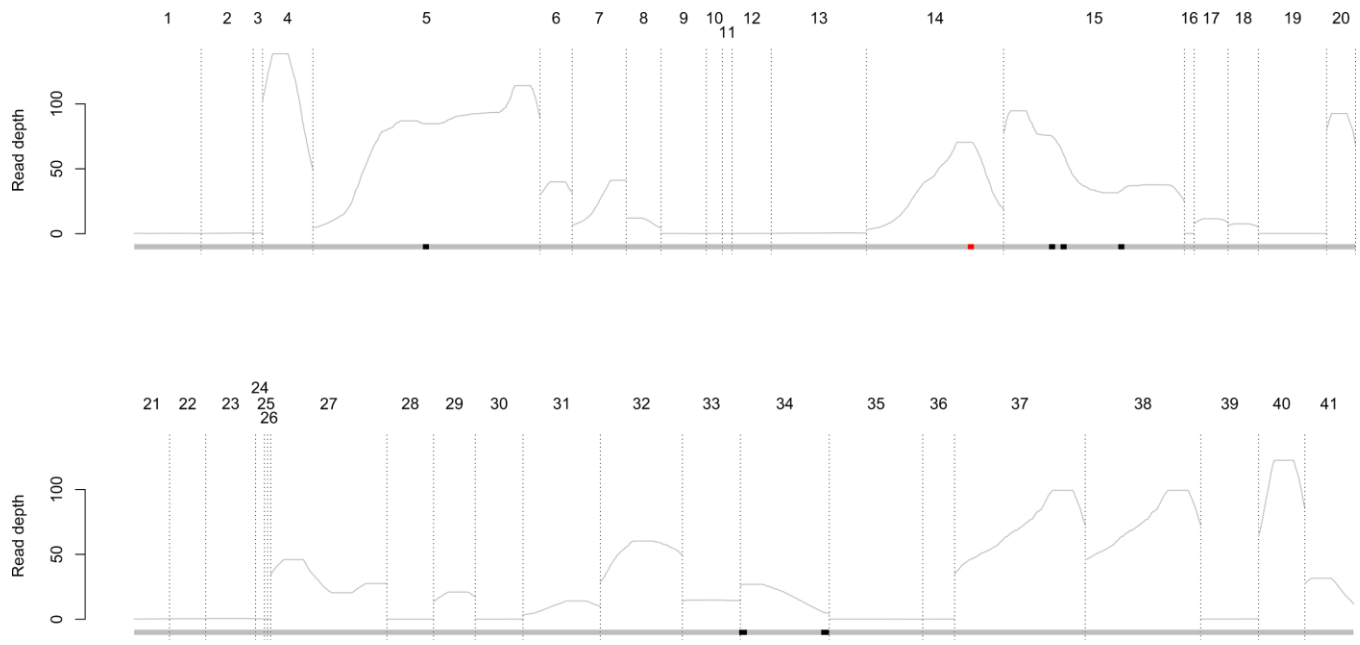



**Fig. 8. *Sm.TRPM$_{PZQ}$* gene: average exon read depth and identified mutations in field samples.** Exons are numbered and delimited with dotted lines. Black boxes on the grey line represent positions of the high frequency mutations. Red box represents the position of the low frequency resistant mutation.

bioRxiv preprint doi: https://doi.org/10.1101/2021.06.09.447779; this version posted June 10, 2021. The copyright holder for this preprint (which was not certified by peer review) is the author/funder, who has granted bioRxiv a license to display the preprint in perpetuity. It is made available under aCC-BY-NC 4.0 International license.

sequencing from 259 miracidia, cercariae or adult parasites from 3 African countries (Senegal, Niger, Tanzania), the Middle East (Oman) and South America (Brazil) *(51, 52)*. We were able to sequence 36/41 exons of *Sm.TRPM$_{PZQ}$* from 122/259 parasites on average (s.e. = 18.65) (Table S3). We found 1 putative PZQ-R SNP in our Illumina reads supported by a very high coverage (Fig. S7). This SNP (c.2708G>T on isoform 5, p.G903*) was found in a single Omani sample and resulted in a truncated protein predicted to result in loss-of-function, demonstrating that PZQ-R alleles are present in natural populations. However, this PZQ-R allele observed was rare and present in heterozygous state so would not impact PZQ response (Fig. 8).

## DISCUSSION

Our genetic approach to determining the genes underlying PZQ resistance – using GWAS and a simple lactate-based read out to determine parasite recovery following PZQ treatment in individual parasites – robustly identifies a TRPM channel (*Sm.TRPM$_{PZQ}$*) as the cause of variation in PZQ response. We were further able to purify SmLE-PZQ-ER and SmLE-PZQ-ES parasites to examine drug response and gene expression and to use chemical blockers to directly implicate *Sm.TRPM$_{PZQ}$*. Our results complement those of Park *et al. (21)* who used a pharmacological approach to determine that *Sm.TRPM$_{PZQ}$* is the major target for PZQ, and identified the critical residues necessary for activation by PZQ. Together, these approaches demonstrate that TRPM is a key determinant of schistosome response to PZQ.

A striking feature of the results is the strength of the PZQ-R phenotype. While previous authors have described quite modest differences (3-5 fold) in PZQ-response among *S. mansoni* isolates *(28, 29)*, this study revealed at least 377-fold difference in $IC_{50}$ between SmLE-PZQ-ER and SmLE-PZQ-ES parasites. These large differences were only evident after we used marker-assisted selection to divide a mixed genotype laboratory *S. mansoni* population into component SmLE-PZQ-ER and SmLE-PZQ-ES populations. The modest $IC_{50}$ differences in previous studies observed are most likely because the parasite

bioRxiv preprint doi: https://doi.org/10.1101/2021.06.09.447779; this version posted June 10, 2021. The copyright holder for this preprint (which was not certified by peer review) is the author/funder, who has granted bioRxiv a license to display the preprint in perpetuity. It is made available under aCC-BY-NC 4.0 International license.

lines compared contained mixed populations of both SmLE-PZQ-ER and SmLE-PZQ-ES individuals. This highlights a critical feature of laboratory schistosome populations that is frequently ignored: these populations are genetically variable and contain segregating genetic and phenotypic variation for a wide variety of parasite traits. In this respect they differ from the clonal bacterial or protozoan parasite "strains" used for laboratory research. Importantly, we can use this segregating genetic variation for genetic mapping of biomedically important parasite traits such as PZQ resistance.

There is strong evidence that PZQ-R parasites occur in schistosome populations in the field, but the contribution of PZQ-R to treatment failure in the field are unclear. Molecular markers are widely used for monitoring changes in drug resistance mutations in malaria parasites *(53–55)* and for evaluating benzimidazole resistance in nematode parasites of veterinary importance *(56, 57)*. The discovery of the genetic basis of resistance to another schistosome drug (oxamniquine) *(58)* now makes genetic surveys possible to evaluate oxamniquine resistance in schistosome populations *(52, 59)*. Identification of *Sm.TRPM*$_{PZQ}$ as a critical determinant of PZQ response, and determination of key residues that can underlie PZQ-R, now makes molecular surveillance possible for *S. mansoni*. We examined variation in *Sm.TRPM*$_{PZQ}$ in 259 parasites collected from locations from across the geographical range of this parasite. We were unable to confirm mutations in any of the key residues that block PZQ binding identified in the mutagenesis studies by Park *et al*. *(21)*. However, we identified a stop codon in a single parasite isolated from a rodent from Oman *(60)* indicating a low frequency of PZQ-R resistance alleles (1/502, frequency = 0.002). This stop codon was in heterozygous state so is unlikely to result in PZQ-R.

These results are extremely encouraging for control programs, but should be viewed with considerable caution for two reasons. First, we do not know yet the regulatory regions of *Sm.TRPM*$_{PZQ}$ and we were unable to identify regulatory variants of *Sm.TRPM*$_{PZQ}$ in this screen. Such variants could reduce expression of *Sm.TRPM*$_{PZQ}$ resulting in PZQ resistance. We note that coding variants underlying PZQ-R phenotype were not found in our laboratory SmLE-PZQ-ER parasites, suggesting that regulatory changes may underlie this trait. Second, *Sm.TRPM*$_{PZQ}$ is a large gene (120 kb and 41 exons) that is poorly captured by genome

bioRxiv preprint doi: https://doi.org/10.1101/2021.06.09.447779; this version posted June 10, 2021. The copyright holder for this preprint (which was not certified by peer review) is the author/funder, who has granted bioRxiv a license to display the preprint in perpetuity. It is made available under aCC-BY-NC 4.0 International license.

sequencing of field samples. We were able to successfully sequence 36/41 exons, including those that directly interact with PZQ *(21)*, using exome capture methods *(51, 52)*. However, improved sequence coverage will be needed for full length sequencing of this gene. Third, the parasite samples we examined did not come from hotspot regions where regular mass drug administration of PZQ has failed to reduce *S. mansoni* burdens *(36, 61)*. Targeted sequencing of miracidia from these populations will be extremely valuable to determine if there are local elevations in $Sm.TRPM_{PZQ}$ variants, or if particular variants are enriched in parasites surviving PZQ treatment. Ideally, such sequence surveys should be partnered with functional validation studies in which variant $Sm.TRPM_{PZQ}$ are expressed in HEK293 cells to determine their response to PZQ exposure *(21)*.

## MATERIALS AND METHODS

### Study design

This study was designed to determine the genetic basis of PZQ-R, and was stimulated by the initial observation that a laboratory *S. mansoni* population generated through selection with PZQ contained both PZQ-S and PZQ-R individuals. The project had 6 stages:(i) QTL location. We conducted a genome-wide association study (GWAS). This involved measuring the PZQ-response of individual worms, pooling those showing high levels of resistance and low levels of resistance, sequencing the pools to high read depth, and then identifying the genome regions showing significant differences in allele frequencies between high and low resistance parasites. (ii) Fine mapping of candidate genes. We identified potential candidate genes in these QTL regions, through examination of gene annotations, and exclusion of genes that are not expressed in adults. We also determined whether the loci determining PZQ-R are inherited in a recessive, dominant or co-dominant manner (iii) Marker assisted purification of PZQ-S and PZQ-R parasites. To separate PZQ-R and PZQ-S parasites into “pure” populations, we genotyped larval parasites for genetic markers in the QTL regions and infected rodents with genotypes associated with PZQ-R or PZQ-S. To verify that this

bioRxiv preprint doi: https://doi.org/10.1101/2021.06.09.447779; this version posted June 10, 2021. The copyright holder for this preprint (which was not certified by peer review) is the author/funder, who has granted bioRxiv a license to display the preprint in perpetuity. It is made available under aCC-BY-NC 4.0 International license.

337 approach worked, we then measured the $IC_{50}$ for each of the purified populations. (iv) Characterization of
338 purified SmLE-PZQ-ER and SmLE-PZQ-ES populations. Separation of SmLE-PZQ-ES and SmLE-PZQ-
339 ER parasite populations allowed us to characterize these in more detail. Specifically, we measured
340 expression in juvenile and adult worms of both sexes in both SmLE-PZQ-ES and SmLE-PZQ-ER parasites.
341 We also quantified parasite fitness traits. (v) Functional analysis. We used RNAi and chemical manipulation
342 approaches to modulate activity of candidate genes and determine the impact of PZQ-resistance. We also
343 used transient expression of candidate genes in cultured mammalian cells, to determine the impact of
344 particular SNPs on response to PZQ-exposure. (vi) Survey of PZQ-resistance variants in field collected
345 parasites. Having determined the gene underlying PZQ-R in laboratory parasites, we examined sequence
346 variation in this gene in a field collection of *S. mansoni* parasites collected to examine the frequency of
347 sequence variants predicted to result in PZQ-resistance. Methods are described in detail (File S1) and in
348 brief below.

349 *Ethics statement*

350 This study was performed following the Guide for the Care and Use of Laboratory Animals of the National
351 Institutes of Health. The protocol was approved by the Institutional Animal Care and Use Committee of
352 Texas Biomedical Research Institute (permit number: 1419-MA and 1420-MU). Ethical permission for
353 collection of samples from humans are described in *(51, 52)*.

354

355 **Biomphalaria glabrata s*nails and* Schistosoma mansoni *parasites***

356 We used uninfected inbred 8 - 10 mm albino *Biomphalaria glabrata* snails (line Bg121 *(62)*). The SmLE
357 *S. mansoni* population was originally obtained from an infected patient in Brazil *(63)*. The SmLE-PZQ-R
358 schistosome population was generated by applying a single round of PZQ selection pressure on SmLE
359 parasites at both snail and rodent stages *(26)* and has been maintained in our laboratory since 2014.

360

361 **Drug resistance tests:**

bioRxiv preprint doi: https://doi.org/10.1101/2021.06.09.447779; this version posted June 10, 2021. The copyright holder for this preprint (which was not certified by peer review) is the author/funder, who has granted bioRxiv a license to display the preprint in perpetuity. It is made available under aCC-BY-NC 4.0 International license.

*Dose-response curves to PZQ in SmLE and SmLE-PZQ-R populations*

We initially measured PZQ sensitivity by examining worm motility *(64)* in SmLE and SmLE-PZQ-R parasite populations. Ten adult males from SmLE or SmLE-PZQ-R populations were placed into each well of a 24-well microplate containing 1 mL DMEM complete media *(65)*. We performed control and experimental groups in triplicate (*N*=240 worms/parasite population). We exposed adult worms to PZQ (0, 0.1 0.3, 0.9, 2.7, 8.1, 24.3 and 72.9 µg/mL) for 24h. Worms were washed (3x) in drug-free medium and incubated (37ºC, 5% $CO_2$) for 2 days. The parasites were observed daily for the 5 days and the number of dead worms scored. Worms were defined as "dead" if they showed no movements and became opaque.

*Metabolic assessment of worm viability using L-lactate assay*

We adapted a method for metabolic assessment of worm viability using an L-lactate assay *(44)*. Adult male SmLE-PZQ-R worms were placed individually in 96-well plates containing 100 µm mesh filter insert (Millipore) in 250µL DMEM complete media. We added PZQ (24.3 µg/mL in DMEM complete media) while controls were treated with the same volume of drug diluent DMSO. At 48h post-treatment, the supernatant (125 µL) was collected from each well and immediately stored at -80 °C until processing. We measured lactate levels in the supernatants of *in vitro* treated adult male worms with a colorimetric L-lactate assay kit (Sigma) using 96-well, optical clear-bottom plates (Corning).

## Genome wide association analysis and QTL mapping

*Schistosome infections*

We collected eggs from livers of hamsters infected with SmLE-PZQ-R *(66)* and exposed one thousand Bg121 snails to five miracidia/snail. After 30 days, snails were individually exposed to light to shed cercariae. We exposed eight hamsters to 840 cercariae (4 cercariae/snail) from a batch of 210 shedding snails. We euthanized hamsters after 45 days to collect adult worms.

*Phenotypic selection*

bioRxiv preprint doi: https://doi.org/10.1101/2021.06.09.447779; this version posted June 10, 2021. The copyright holder for this preprint (which was not certified by peer review) is the author/funder, who has granted bioRxiv a license to display the preprint in perpetuity. It is made available under aCC-BY-NC 4.0 International license.

We plated adult SmLE-PZQ-R males individually in 96-well plates (60 worms per plate) in 250 µL of DMEM complete media and treated with a 24.3 µg/mL PZQ. A group of 12 worms was treated with the same volume of drug diluent DMSO. This GWAS experiment was done twice independently. A total of 590 and 691 adult male worms were collected, cultured *in vitro* and exposed to PZQ for the two experiments.

We collected media supernatants (125 µL) in 96-well PCR plates after 24h in culture (pre-treatment) and 48h post-treatment for quantifying lactate levels. We took the 20% of the treated worms releasing the highest amount of lactate (average L-lactate production ± SD: Experiment 1 = 61.44 nmol/h ± 13.16 / Experiment 2 = 56.38 nmol/h ± 10.82) and the 20% of the treated worms releasing the lowest amount of lactate (average L-lactate production ± SD: Experiment 1 = 28.61 nmol/h ± 5.32 / Experiment 2 = 23.04 nmol/h ± 4.14), 48h post PZQ treatment.

*DNA extraction and library preparation*

We sequenced whole genomes of the two pools of recovered (Experiment 1: 116 worms / Experiment 2: 137 worms) and susceptible worms (Experiment 1: 116 worms / Experiment 2: 137 worms) and measured allele frequencies in each pool to identify genome regions showing high differentiation. We extracted gDNA from pools of worms (Blood and Tissue kit, Qiagen) and prepared whole genome libraries in triplicate (KAPA HyperPlus kit, KAPA Biosystems). Raw sequence data are available at the NCBI Sequence Read Archive (PRJNA699326).

*Bioinformatic analysis*

We used Jupyter notebook and scripts used for processing the sequencing data and identifying the QTL (https://github.com/fdchevalier/PZQ-R_DNA).

a. ***Sequence analysis and variant calling***

We (i) aligned the sequencing data against the *S. mansoni* reference genome using BWA *(67)* and SAMtools *(68)*, (ii) used GATK *(69, 70)* to mark PCR duplicates and recalibrate base scores, (iii) used the

bioRxiv preprint doi: https://doi.org/10.1101/2021.06.09.447779; this version posted June 10, 2021. The copyright holder for this preprint (which was not certified by peer review) is the author/funder, who has granted bioRxiv a license to display the preprint in perpetuity. It is made available under aCC-BY-NC 4.0 International license.

HaplotypeCaller module of GATK to call variants (SNP/indel) and GenotypeGVCFs module to perform joint genotyping. We merged VCF files using the MergeVcfs module. All steps were automated using Snakemake *(71)*.

b. ***QTL identification***

We examined the difference in allele frequencies between low and high lactate parasites across the genome by calculating a *Z*-score at each bi-allelic site. We weighed *Z*-scores by including the number of worms in each treatment and the difference in the total read depth across the triplicated libraries of each treatment at the given variant. We combined *Z*-scores generated from each biological replicate. Bonferroni correction was calculated with $\alpha = 0.05$.

**Relationship between worm genotype at chr. 2 and 3 and PZQ-R phenotype**

To validate the impact of worm genotypes on PZQ resistance phenotype and to determine whether PZQ-R shows recessive, dominant or codominant inheritance, we measured the PZQ-R phenotype of individual worms, and genotyped worms for markers at the peak of the QTLs located.

*Measuring PZQ-R in individual worms*

We plated 120 SmLE-PZQ-R adult male worms individually in 96-well plates, treated them with PZQ (24.3 µg/mL) and collected media supernatants pre- (24 h) and post- (48 h) treatment, and used L-lactate assays to determine PZQ-R status. We extracted gDNA from each worm individually *(66)*.

*PCR-RFLP for chr.2 and chr.3 loci*

We used PCR-RFLP to genotype single worms at loci marking QTL peaks on chr. 2 (C>A, chr SM_V7_2: 1072148) and chr. 3 (T>C, chr SM_V7_3: 741987) (Table S4). We digested PCR amplicons for chr. 2 with BslI (NEB) and chr. 3 with Mse1 (NEB), and visualized digested PCR amplicons by 2% agarose gel electrophoresis.

bioRxiv preprint doi: https://doi.org/10.1101/2021.06.09.447779; this version posted June 10, 2021. The copyright holder for this preprint (which was not certified by peer review) is the author/funder, who has granted bioRxiv a license to display the preprint in perpetuity. It is made available under aCC-BY-NC 4.0 International license.

*Quantitative PCR of copy number variation (CNV) in single worms*

We genotyped individual worms for a deletion on chr. 3 (position 1220683-1220861 bp) using a qPCR assay. Methods and primers are described in Table S4.

## Marker assisted selection of resistant and susceptible parasite populations

*Selection of SmLE-PZQ-ER and SmLE-PZQ-ES populations*

We separated the polymorphic SmLE-PZQ-R schistosome population based on chr. 3 QTL genotype using PCR-RFLP. We exposed 960 inbred *B. glabrata* Bg121 snails to one miracidium SmLE-PZQ-R *(66)*. At four weeks post-exposure, we identified infected snails (*N*=272), collected cercariae from individual snails, extracted cercarial DNA *(66)*), and genotyped each parasite for the chr. 3 locus using PCR-RFLP (Homozygous R/R: n=89 – 36%; Homozygous S/S: n=39 – 16%; Heterozygous R/S: n=117 – 49%), and determined their gender by PCR *(72)*. We selected 32 R/R parasites and 32 S/S genotypes. For both R/R and S/S we used 13 males and 19 females. We exposed 5 hamsters to 800 cercariae of 32 R/R genotypes parasites and 5 hamsters to 800 cercariae 32 S/S genotyped parasites. This single generation marker assisted selection procedure generates two subpopulations: SmLE-PZQ-ER is enriched for parasites with R/R genotype, while SmLE-PZQ-ES is enriched for S/S genotypes.

*PZQ $IC_{50}$ with SmLE-PZQ-ER and SmLE-PZQ-ES*

Forty-five days after infection, we euthanized and perfused hamsters to recover adult schistosome worms for SmLE-PZQ-ER and SmLE-PZQ-ES subpopulations. We placed adult males in 96-well plates and cultured in 250 µL DMEM complete media. We determined PZQ dose-response for both SmLE-PZQ-ER and SmLE-PZQ-ES population.

*gDNA extraction and library preparation and bioinformatics*

We recovered the F1 SmLE-PZQ-ER and SmLE-PZQ-ES worms and extracted gDNA from pools of adult males or females separately. We prepared whole genome libraries from these pools in triplicate using the

bioRxiv preprint doi: https://doi.org/10.1101/2021.06.09.447779; this version posted June 10, 2021. The copyright holder for this preprint (which was not certified by peer review) is the author/funder, who has granted bioRxiv a license to display the preprint in perpetuity. It is made available under aCC-BY-NC 4.0 International license.

KAPA HyperPlus kit (KAPA Biosystems). Sequence data are available at the NCBI Sequence Read Archive (accession numbers PRJNA701978). The analysis was identical to the GWAS and QTL mapping analysis (see Jupyter notebook and scripts (https://github.com/fdchevalier/PZQ-R_DNA)).

**Transcriptomic analysis of resistant and susceptible schistosome worms at juvenile and adult stages**

*Sample collection*

We recovered *S. mansoni* SmLE-PZQ-ER and SmLE-PZQ-ES worms by perfusion from hamsters at 28 days (juveniles) or 45 days (adults) post-infection. For each subpopulation, (SmLE-PZQ-ER or SmLE-PZQ-ES), we collected 3 biological replicates of 30 males or 30 females for the 28d juvenile worms, and 3 biological replicates of 30 males or 60 females for the 45d adult worms.

*RNA extraction and RNAseq library preparation*

***a. RNA extraction***

We extracted total RNA from all the *S. mansoni* adult and juvenile worms (RNeasy Mini kit, Qiagen), quantified the RNA recovered (Qubit RNA Assay Kit, Invitrogen) and assessed the RNA integrity by TapeStation (Agilent - RNA integrity numbers: ~8.5–10 for all samples).

***b. RNAseq library preparation***

We prepared RNAseq libraries using the KAPA Stranded mRNA-seq kit (KAPA Biosystems) using 500ng RNA for each library. We sequenced the libraries using 150 bp pair-end reads. Raw sequence data are available at the NCBI Sequence Read Archive (accession numbers PRJNA704646).

***c. Bioinformatic analysis.***

To identify differentially expressed genes, we aligned the sequencing data against the *S. mansoni* reference genome using STAR. We quantified gene and isoform abundances by computing transcripts per million values using RSEM and compared abundances between groups (ES/ER, males/females, juveniles/adults) using the R package EBSeq.

bioRxiv preprint doi: https://doi.org/10.1101/2021.06.09.447779; this version posted June 10, 2021. The copyright holder for this preprint (which was not certified by peer review) is the author/funder, who has granted bioRxiv a license to display the preprint in perpetuity. It is made available under aCC-BY-NC 4.0 International license.

**Manipulation of *Sm.TRPM$_{PZQ}$* channel expression or function:**

*RNA interference*

We attempted RNA interference to functionally validate the implication of *Sm.TRPM$_{PZQ}$* on schistosome PZQ resistance. The methods used are described in File S1 and Table S2, but were unsuccessful so are not described here.

*Specific Sm.TRPM$_{PZQ}$ chemical inhibitor and activators*

We used specific chemical inhibitor and activators (Chulkov *et al.*, in prep) to manipulate the function of Sm.TRPM$_{PZQ}$ to examine the impact on PZQ-response. We placed individual SmLE-PZQ-ER and SmLE-PZQ-ES adult male worms in 96-well plates containing DMEM complete media. After 24h, 20 worms from each population were treated either with a cocktail combining PZQ (1 µg/mL) and i) 50 µM of *Sm.TRPM$_{PZQ}$* blocker (MB2) or ii) 10 µM, 25 µM or 50 µM of *Sm.TRPM$_{PZQ}$* activator (MV1) respectively or iii) drug diluent (DMSO). We also set up control plates to evaluate the impact of *Sm.TRPM$_{PZQ}$* blocker or activator alone. Worms were exposed to these drug cocktails for 24h, washed 3 times with drug-free medium, and incubated (37ºC,5% $CO_2$) for 2 days. We collected media supernatants (125µL) before treatment (after 24h in culture) and 48h post-treatment and quantified lactate levels.

***In vivo* parasite survival after PZQ treatment**

We split 24 female Balb/C mice into two groups: one group exposed by tail immersion to SmLE-PZQ-ER (80 cercariae/mouse from 40 infected snails) and the second one to SmLE-PZQ-ES (80 cercariae/mouse from 40 infected snails). Forty days post-infection, we treated mice by oral gavage with either 120mg/kg of PZQ (1% DMSO + vegetable oil in a total volume of 150 µL) or the same volume of drug diluent only (control group). We euthanized and perfused *(65)* mice (day 50 post-infection) to recover worms.

***Sm.TRPM$_{PZQ}$* variants in *S. mansoni* field samples**

bioRxiv preprint doi: https://doi.org/10.1101/2021.06.09.447779; this version posted June 10, 2021. The copyright holder for this preprint (which was not certified by peer review) is the author/funder, who has granted bioRxiv a license to display the preprint in perpetuity. It is made available under aCC-BY-NC 4.0 International license.

*Variants identification in exome-sequenced data from natural* S. mansoni *parasites*

We utilized exome sequence data from *S. mansoni* from Africa, South America and the middle East to investigate variation in *Sm.TRPM*$_{PZQ}$. African miracidia were from the Schistosomiasis collection at the Natural History Museum (SCAN) *(73)*, Brazilian miracidia and Omani cercariae and adult worms were collected previously. We have previously described exome sequencing methods for *S. mansoni (51, 52)*. Data were analyzed the same way as described in Chevalier et al. *(52)*. Code is available in Jupyter notebook and scripts associated (https://github.com/fdchevalier/PZQ-R_field).

*Sanger re-sequencing to confirm the presence of the* Sm.TRPM$_{PZQ}$ *field variants*

To confirm the presence of variants in *Sm.TRPM*$_{PZQ}$ (when read depth was <10 reads), we performed Sanger re-sequencing of mutations of interest close to the PZQ binding site *(21)*. Primers and conditions are listed in Table S4. We scored variants using PolyPhred software (v6.18) (Nickerson et al., 1997). Sequences are deposited in GenBank (KU951903-KU952091).

## Statistical analysis

Statistical analyzes and graphs were performed using R software (v3.5.1) *(74)*. We used the drc package from R to analyze dose-response datasets and Readqpcr and Normqpcr packages to analyze RT-qPCR datasets. For non-normal data (Shapiro test, $p < 0.05$), we used Chi-square test, Kruskal-Wallis test followed by pairwise Wilcoxon-Mann-Whitney post-hoc test or a Wilcoxon-Mann-Whitney test. For normal data, we used one–way ANOVA or a pairwise comparison Welsh *t*-test. The confidence intervals were set to 95% and *p*-values < 0.05 were considered significant.

## Supplementary Materials

Fig. S1. Development of a lactate assay for assaying worm recovery.

bioRxiv preprint doi: https://doi.org/10.1101/2021.06.09.447779; this version posted June 10, 2021. The copyright holder for this preprint (which was not certified by peer review) is the author/funder, who has granted bioRxiv a license to display the preprint in perpetuity. It is made available under aCC-BY-NC 4.0 International license.

Fig. S2. Validation of marker-assisted selection of SmLE-PZQ-ER and ES using Next Generation Sequencing (NGS).

Fig. S3. Large deletions adjacent to *Sm.TRPM*$_{PZQ}$ and SOX13 transcription factor.

Fig. S4. Detailed genes and isoforms expression in SmLE-PZQ-ER and SmLE-PZQ-ES parasites.

Fig. S5. Cellular localization of *Sm.TRPM*$_{PZQ}$ expression in *S. mansoni*.

Fig. S6. Impact of *in vivo* PZQ treatment on SmLE-PZQ-ER and SmLE-PZQ-ES parasites.

Fig. S7. Stop codon identified in *S. mansoni* field sample from Oman.

Table S1. Genes in QTL regions on chr. 2 and 3.

Table S2. Details of RNAi for *Sm.TRPM*$_{PZQ.}$

Table S3. Mutations present in *Sm.TRPM*$_{PZQ}$ in natural schistosome populations from 3 African countries (Senegal, Niger, Tanzania), the Middle East (Oman) and South America (Brazil).

Table S4. Summary table of siRNA sequences and primer sequences used for PCR-RFLP, RT-qPCR, PCRs and Sanger sequencing.

File S1. Expanded Material and Methods.

bioRxiv preprint doi: https://doi.org/10.1101/2021.06.09.447779; this version posted June 10, 2021. The copyright holder for this preprint (which was not certified by peer review) is the author/funder, who has granted bioRxiv a license to display the preprint in perpetuity. It is made available under aCC-BY-NC 4.0 International license.

## References and Notes

1. World Health Organization, Schistosomiasis, (available at https://www.who.int/news-room/fact-sheets/detail/schistosomiasis).

2. G. B. D. 2017 Disease, I. Incidence, P. Collaborators, Global, regional, and national incidence, prevalence, and years lived with disability for 354 diseases and injuries for 195 countries and territories, 1990-2017: a systematic analysis for the Global Burden of Disease Study 2017., *Lancet (London, England)* **392**, 1789–1858 (2018).

3. D. P. McManus, D. W. Dunne, M. Sacko, J. Utzinger, B. J. Vennervald, X.-N. Zhou, Schistosomiasis., *Nature reviews. Disease primers* **4**, 13 (2018).

4. G. B. D. 2015 Mortality, C. of Death Collaborators, Global, regional, and national life expectancy, all-cause mortality, and cause-specific mortality for 249 causes of death, 1980-2015: a systematic analysis for the Global Burden of Disease Study 2015., *Lancet (London, England)* **388**, 1459–1544 (2016).

5. M. A. Verjee, Schistosomiasis: Still a cause of significant morbidity and mortality., *Research and reports in tropical medicine* **10**, 153–163 (2019).

6. M. J. van der Werf, S. J. de Vlas, S. Brooker, C. W. N. Looman, N. J. D. Nagelkerke, J. D. F. Habbema, D. Engels, Quantification of clinical morbidity associated with schistosome infection in sub-Saharan Africa., *Acta Trop* **86**, 125–139 (2003).

7. W. H. Organization, others, Schistosomiasis: progress report 2001-2011, strategic plan 2012-2020, (2013).

8. A. K. Deol, F. M. Fleming, B. Calvo-Urbano, M. Walker, V. Bucumi, I. Gnandou, E. M. Tukahebwa, S. Jemu, U. J. Mwingira, A. Alkohlani, M. Traoré, E. Ruberanziza, S. Touré, M.-G. Basáñez, M. D. French, J. P. Webster, Schistosomiasis - assessing progress toward the 2020 and 2025 global goals., *The New England journal of medicine* **381**, 2519–2528 (2019).

9. S. H. Xiao, P. A. Friedman, B. A. Catto, L. T. Webster, Praziquantel-induced vesicle formation in the tegument of male Schistosoma mansoni is calcium dependent., *The Journal of parasitology* **70**, 177–179 (1984).

10. R. Pax, J. L. Bennett, R. Fetterer, A benzodiazepine derivative and praziquantel: effects on musculature of Schistosoma mansoni and Schistosoma japonicum., *Naunyn-Schmiedeberg's archives of pharmacology* **304**, 309–315 (1978).

11. B. Becker, H. Mehlhorn, P. Andrews, H. Thomas, J. Eckert, Light and electron microscopic studies on the effect of praziquantel on Schistosoma mansoni, Dicrocoelium dendriticum, and Fasciola hepatica (Trematoda) in vitro., *Zeitschrift fur Parasitenkunde (Berlin, Germany)* **63**, 113–128 (1980).

12. C. S. Bricker, J. W. Depenbusch, J. L. Bennett, D. P. Thompson, The relationship between tegumental disruption and muscle contraction in Schistosoma mansoni exposed to various compounds., *Zeitschrift fur Parasitenkunde (Berlin, Germany)* **69**, 61–71 (1983).

13. P. M. Cupit, C. Cunningham, What is the mechanism of action of praziquantel and how might resistance strike?, *Future medicinal chemistry* **7**, 701–705 (2015).

14. C. M. Thomas, D. J. Timson, The mechanism of action of praziquantel: Six hypotheses., *Current topics in medicinal chemistry* **18**, 1575–1584 (2018).

15. A. B. Kohn, P. A. Anderson, J. M. Roberts-Misterly, R. M. Greenberg, Schistosome calcium channel beta subunits. Unusual modulatory effects and potential role in the action of the antischistosomal drug praziquantel., *The Journal of biological chemistry* **276**, 36873–36876 (2001).

bioRxiv preprint doi: https://doi.org/10.1101/2021.06.09.447779; this version posted June 10, 2021. The copyright holder for this preprint (which was not certified by peer review) is the author/funder, who has granted bioRxiv a license to display the preprint in perpetuity. It is made available under aCC-BY-NC 4.0 International license.

595 16. M. C. Jeziorski, R. M. Greenberg, Voltage-gated calcium channel subunits from platyhelminths: potential role in
596 praziquantel action., *International journal for parasitology* **36**, 625–632 (2006).

597 17. J. D. Chan, M. Zarowiecki, J. S. Marchant, $Ca^{2+}$ channels and praziquantel: a view from the free world.,
598 *Parasitology international* **62**, 619–628 (2013).

599 18. R. S. Kasinathan, L. K. Sharma, C. Cunningham, T. R. Webb, R. M. Greenberg, Inhibition or knockdown of
600 ABC transporters enhances susceptibility of adult and juvenile schistosomes to Praziquantel., *PLoS neglected*
601 *tropical diseases* **8**, e3265 (2014).

602 19. R. M. Greenberg, ABC multidrug transporters in schistosomes and other parasitic flatworms., *Parasitology*
603 *international* **62**, 647–653 (2013).

604 20. S.-K. Park, G. S. Gunaratne, E. G. Chulkov, F. Moehring, P. McCusker, P. I. Dosa, J. D. Chan, C. L. Stucky, J.
605 S. Marchant, The anthelmintic drug praziquantel activates a schistosome transient receptor potential channel., *The*
606 *Journal of biological chemistry* **294**, 18873–18880 (2019).

607 21. S.-K. Park, L. Friedrich, N. A. Yahya, C. Rohr, E. G. Chulkov, D. Maillard, F. Rippmann, T. Spangenberg, J. S.
608 Marchant, Mechanism of praziquantel action at a parasitic flatworm ion channel, *bioRxiv* (2021),
609 doi:10.1101/2021.03.09.434291.

610 22. P. G. Fallon, M. J. Doenhoff, Drug-resistant schistosomiasis: resistance to praziquantel and oxamniquine
611 induced in *Schistosoma mansoni* in mice is drug specific., *Am J Trop Med Hyg* **51**, 83–88 (1994).

612 23. B. Gryseels, L. Nkulikyinka, D. Engels, Impact of repeated community-based selective chemotherapy on
613 morbidity due to schistosomiasis mansoni., *The American journal of tropical medicine and hygiene* **51**, 634–641
614 (1994).

615 24. M. Ismail, S. Botros, A. Metwally, S. William, A. Farghally, L. F. Tao, T. A. Day, J. L. Bennett, Resistance to
616 praziquantel: direct evidence from Schistosoma mansoni isolated from Egyptian villagers., *The American journal of*
617 *tropical medicine and hygiene* **60**, 932–935 (1999).

618 25. D. Alonso, J. Muñoz, J. Gascón, M. E. Valls, M. Corachan, Failure of standard treatment with praziquantel in
619 two returned travelers with Schistosoma haematobium infection., *The American journal of tropical medicine and*
620 *hygiene* **74**, 342–344 (2006).

621 26. F. F. B. Couto, P. M. Z. Coelho, N. Araújo, J. R. Kusel, N. Katz, L. K. Jannotti-Passos, A. C. A. Mattos,
622 Schistosoma mansoni: a method for inducing resistance to praziquantel using infected Biomphalaria glabrata snails.,
623 *Memorias do Instituto Oswaldo Cruz* **106**, 153–157 (2011).

624 27. W. Wang, L. Wang, Y.-S. Liang, Susceptibility or resistance of praziquantel in human schistosomiasis: a
625 review., *Parasitology research* **111**, 1871–1877 (2012).

626 28. D. Cioli, S. S. Botros, K. Wheatcroft-Francklow, A. Mbaye, V. Southgate, L.-A. T. Tchuenté, L. Pica-Mattoccia,
627 A. R. Troiani, S. H. S. El-Din, A.-N. A. Sabra, J. Albin, D. Engels, M. J. Doenhoff, Determination of ED50 values
628 for praziquantel in praziquantel-resistant and -susceptible Schistosoma mansoni isolates., *International journal for*
629 *parasitology* **34**, 979–987 (2004).

630 29. L. Pica-Mattoccia, M. J. Doenhoff, C. Valle, A. Basso, A.-R. Troiani, P. Liberti, A. Festucci, A. Guidi, D. Cioli,
631 Genetic analysis of decreased praziquantel sensitivity in a laboratory strain of *Schistosoma mansoni*., *Acta Trop* **111**,
632 82–85 (2009).

633 30. J. Zwang, P. Olliaro, Efficacy and safety of praziquantel 40 mg/kg in preschool-aged and school-aged children: a
634 meta-analysis., *Parasites & vectors* **10**, 47 (2017).

bioRxiv preprint doi: https://doi.org/10.1101/2021.06.09.447779; this version posted June 10, 2021. The copyright holder for this preprint (which was not certified by peer review) is the author/funder, who has granted bioRxiv a license to display the preprint in perpetuity. It is made available under aCC-BY-NC 4.0 International license.

31. L. Pica-Mattoccia, D. Cioli, Sex- and stage-related sensitivity of Schistosoma mansoni to in vivo and in vitro praziquantel treatment., *International journal for parasitology* **34**, 527–533 (2004).

32. S. Botros, L. Pica-Mattoccia, S. William, N. El-Lakkani, D. Cioli, Effect of praziquantel on the immature stages of Schistosoma haematobium., *International journal for parasitology* **35**, 1453–1457 (2005).

33. M. Ismail, A. Metwally, A. Farghaly, J. Bruce, L. F. Tao, J. L. Bennett, Characterization of isolates of Schistosoma mansoni from Egyptian villagers that tolerate high doses of praziquantel., *The American journal of tropical medicine and hygiene* **55**, 214–218 (1996).

34. S. D. Melman, M. L. Steinauer, C. Cunningham, L. S. Kubatko, I. N. Mwangi, N. B. Wynn, M. W. Mutuku, D. M. S. Karanja, D. G. Colley, C. L. Black, W. E. Secor, G. M. Mkoji, E. S. Loker, Reduced susceptibility to praziquantel among naturally occurring Kenyan isolates of Schistosoma mansoni., *PLoS neglected tropical diseases* **3**, e504 (2009).

35. S. William, S. Botros, M. Ismail, A. Farghally, T. A. Day, J. L. Bennett, Praziquantel-induced tegumental damage in vitro is diminished in schistosomes derived from praziquantel-resistant infections., *Parasitology* **122 Pt 1**, 63–66 (2001).

36. N. Kittur, C. H. Campbell, S. Binder, Y. Shen, R. E. Wiegand, J. R. Mwanga, S. M. Kinung'hi, R. M. Musuva, M. R. Odiere, S. H. Matendechero, S. Knopp, D. G. Colley, Discovering, defining, and summarizing persistent hotspots in SCORE studies., *The American journal of tropical medicine and hygiene* **103**, 24–29 (2020).

37. P. A. Mawa, J. Kincaid-Smith, E. M. Tukahebwa, J. P. Webster, S. Wilson, Schistosomiasis morbidity hotspots: Roles of the human host, the parasite and their interface in the development of severe morbidity., *Frontiers in immunology* **12**, 635869 (2021).

38. T. Crellen, M. Walker, P. H. L. Lamberton, N. B. Kabatereine, E. M. Tukahebwa, J. A. Cotton, J. P. Webster, Reduced efficacy of praziquantel against schistosoma mansoni is associated with multiple rounds of mass drug administration., *Clinical infectious diseases : an official publication of the Infectious Diseases Society of America* **63**, 1151–1159 (2016).

39. A. V. Protasio, I. J. Tsai, A. Babbage, S. Nichol, M. Hunt, M. A. Aslett, N. De Silva, G. S. Velarde, T. J. C. Anderson, R. C. Clark, C. Davidson, G. P. Dillon, N. E. Holroyd, P. T. LoVerde, C. Lloyd, J. McQuillan, G. Oliveira, T. D. Otto, S. J. Parker-Manuel, M. A. Quail, R. A. Wilson, A. Zerlotini, D. W. Dunne, M. Berriman, A systematically improved high quality genome and transcriptome of the human blood fluke *Schistosoma mansoni*., *PLoS Negl Trop Dis* **6**, e1455 (2012).

40. T. J. C. Anderson, P. T. LoVerde, W. Le Clec'h, F. D. Chevalier, Genetic crosses and linkage mapping in schistosome parasites., *Trends Parasitol* **34**, 982–996 (2018).

41. S. K. Volkman, J. Herman, A. K. Lukens, D. L. Hartl, Genome-wide association studies of drug-resistance determinants., *Trends in parasitology* **33**, 214–230 (2017).

42. J. Wit, C. M. Dilks, E. C. Andersen, Complementary approaches with free-living and parasitic nematodes to understanding anthelmintic resistance., *Trends in parasitology* **37**, 240–250 (2021).

43. R. H. Fetterer, R. A. Pax, J. L. Bennett, Praziquantel, potassium and 2,4-dinitrophenol: analysis of their action on the musculature of Schistosoma mansoni., *European journal of pharmacology* **64**, 31–38 (1980).

44. S. Howe, D. Zöphel, H. Subbaraman, C. Unger, J. Held, T. Engleitner, W. H. Hoffmann, A. Kreidenweiss, Lactate as a novel quantitative measure of viability in Schistosoma mansoni drug sensitivity assays., *Antimicrobial agents and chemotherapy* **59**, 1193–1199 (2015).

bioRxiv preprint doi: https://doi.org/10.1101/2021.06.09.447779; this version posted June 10, 2021. The copyright holder for this preprint (which was not certified by peer review) is the author/funder, who has granted bioRxiv a license to display the preprint in perpetuity. It is made available under aCC-BY-NC 4.0 International license.

675 45. M. Girardot, E. Bayet, J. Maurin, P. Fort, P. Roux, P. Raynaud, SOX9 has distinct regulatory roles in alternative
676 splicing and transcription., *Nucleic acids research* **46**, 9106–9118 (2018).

677 46. G. Wendt, L. Zhao, R. Chen, C. Liu, A. J. O'Donoghue, C. R. Caffrey, M. L. Reese, J. J. Collins, A single-cell
678 RNA-seq atlas of , javax.xml.bind.JAXBElement@463bbb2c, identifies a key regulator of blood feeding., *Science*
679 *(New York, N.Y.)* **369**, 1644–1649 (2020).

680 47. S. William, A. Sabra, F. Ramzy, M. Mousa, Z. Demerdash, J. L. Bennett, T. A. Day, S. Botros, Stability and
681 reproductive fitness of Schistosoma mansoni isolates with decreased sensitivity to praziquantel., *International*
682 *journal for parasitology* **31**, 1093–1100 (2001).

683 48. S. Hernando-Amado, F. Sanz-García, P. Blanco, J. L. Martínez, Fitness costs associated with the acquisition of
684 antibiotic resistance., *Essays in biochemistry* **61**, 37–48 (2017).

685 49. P. Durão, R. Balbontín, I. Gordo, Evolutionary mechanisms shaping the maintenance of antibiotic resistance.,
686 *Trends in microbiology* **26**, 677–691 (2018).

687 50. S. Nair, X. Li, G. A. Arya, M. McDew-White, M. Ferrari, F. Nosten, T. J. C. Anderson, Fitness costs and the
688 rapid spread of , javax.xml.bind.JAXBElement@527e161e, -C580Y substitutions conferring artemisinin resistance.,
689 *Antimicrobial agents and chemotherapy* **62** (2018), doi:10.1128/AAC.00605-18.

690 51. W. Le Clec'h, F. D. Chevalier, M. McDew-White, F. Allan, B. L. Webster, A. N. Gouvras, S. Kinunghi, L.-A.
691 Tchuem Tchuenté, A. Garba, K. A. Mohammed, S. M. Ame, J. P. Webster, D. Rollinson, A. M. Emery, T. J. C.
692 Anderson, Whole genome amplification and exome sequencing of archived schistosome miracidia., *Parasitology*
693 **145**, 1739–1747 (2018).

694 52. F. D. Chevalier, W. Le Clec'h, M. McDew-White, V. Menon, M. A. Guzman, S. P. Holloway, X. Cao, A. B.
695 Taylor, S. Kinung'hi, A. N. Gouvras, B. L. Webster, J. P. Webster, A. M. Emery, D. Rollinson, A. Garba Djirmay,
696 K. M. Al Mashikhi, S. Al Yafae, M. A. Idris, H. Moné, G. Mouahid, P. J. Hart, P. T. LoVerde, T. J. C. Anderson,
697 Oxamniquine resistance alleles are widespread in Old World Schistosoma mansoni and predate drug deployment.,
698 *PLoS pathogens* **15**, e1007881 (2019).

699 53. D. Ménard, N. Khim, J. Beghain, A. A. Adegnika, M. Shafiul-Alam, O. Amodu, G. Rahim-Awab, C. Barnadas,
700 A. Berry, Y. Boum, M. D. Bustos, J. Cao, J.-H. Chen, L. Collet, L. Cui, G.-D. Thakur, A. Dieye, D. Djallé, M. A.
701 Dorkenoo, C. E. Eboumbou-Moukoko, F.-E.-C. J. Espino, T. Fandeur, M.-F. Ferreira-da-Cruz, A. A. Fola, H.-P.
702 Fuehrer, A. M. Hassan, S. Herrera, B. Hongvanthong, S. Houzé, M. L. Ibrahim, M. Jahirul-Karim, L. Jiang, S.
703 Kano, W. Ali-Khan, M. Khanthavong, P. G. Kremsner, M. Lacerda, R. Leang, M. Leelawong, M. Li, K. Lin, J.-B.
704 Mazarati, S. Ménard, I. Morlais, H. Muhindo-Mavoko, L. Musset, K. Na-Bangchang, M. Nambozi, K. Niaré, H.
705 Noedl, J.-B. Ouédraogo, D. R. Pillai, B. Pradines, B. Quang-Phuc, M. Ramharter, M. Randrianarivelojosia, J.
706 Sattabongkot, A. Sheikh-Omar, K. D. Silué, S. B. Sirima, C. Sutherland, D. Syafruddin, R. Tahar, L.-H. Tang, O. A.
707 Touré, P. Tshibangu-wa-Tshibangu, I. Vigan-Womas, M. Warsame, L. Wini, S. Zakeri, S. Kim, R. Eam, L. Berne,
708 C. Khean, S. Chy, M. Ken, K. Loch, L. Canier, V. Duru, E. Legrand, J.-C. Barale, B. Stokes, J. Straimer, B.
709 Witkowski, D. A. Fidock, C. Rogier, P. Ringwald, F. Ariey, O. Mercereau-Puijalon, K. A. R. M. A. Consortium, A
710 worldwide map of plasmodium falciparum k13-propeller polymorphisms., *The New England journal of medicine*
711 **374**, 2453–2464 (2016).

712 54. M. Mayxay, S. Nair, D. Sudimack, M. Imwong, N. Tanomsing, T. Pongvongsa, S. Phompida, R. Phetsouvanh,
713 N. J. White, T. J. C. Anderson, P. N. Newton, Combined molecular and clinical assessment of Plasmodium
714 falciparum antimalarial drug resistance in the Lao People's Democratic Republic (Laos)., *The American journal of*
715 *tropical medicine and hygiene* **77**, 36–43 (2007).

716 55. T. O. Apinjoh, A. Ouattara, V. P. K. Titanji, A. Djimde, A. Amambua-Ngwa, Genetic diversity and drug
717 resistance surveillance of Plasmodium falciparum for malaria elimination: is there an ideal tool for resource-limited
718 sub-Saharan Africa?, *Malaria journal* **18**, 217 (2019).

bioRxiv preprint doi: https://doi.org/10.1101/2021.06.09.447779; this version posted June 10, 2021. The copyright holder for this preprint (which was not certified by peer review) is the author/funder, who has granted bioRxiv a license to display the preprint in perpetuity. It is made available under aCC-BY-NC 4.0 International license.

719 56. A. C. Kotze, R. K. Prichard, Anthelmintic resistance in haemonchus contortus: History, mechanisms and
720 diagnosis., *Advances in parasitology* **93**, 397–428 (2016).

721 57. L. A. Melville, E. Redman, A. A. Morrison, P. C. Rebecca Chen, R. Avramenko, S. Mitchell, J. Van Dijk, G.
722 Innocent, F. Sargison, C. Aitken, J. S. Gilleard, D. J. Bartley, Large scale screening for benzimidazole resistance
723 mutations in Nematodirus battus, using both pyrosequence genotyping and deep amplicon sequencing, indicates the
724 early emergence of resistance on UK sheep farms., *International journal for parasitology. Drugs and drug*
725 *resistance* **12**, 68–76 (2020).

726 58. C. L. L. Valentim, D. Cioli, F. D. Chevalier, X. Cao, A. B. Taylor, S. P. Holloway, L. Pica-Mattoccia, A. Guidi,
727 A. Basso, I. J. Tsai, M. Berriman, C. Carvalho-Queiroz, M. Almeida, H. Aguilar, D. E. Frantz, P. J. Hart, P. T.
728 LoVerde, T. J. C. Anderson, Genetic and molecular basis of drug resistance and species-specific drug action in
729 schistosome parasites., *Science (New York, N.Y.)* **342**, 1385–1389 (2013).

730 59. F. D. Chevalier, W. Le Clec'h, N. Eng, A. R. Rugel, R. R. de Assis, G. Oliveira, S. P. Holloway, X. Cao, P. J.
731 Hart, P. T. LoVerde, T. J. C. Anderson, Independent origins of loss-of-function mutations conferring oxamniquine
732 resistance in a Brazilian schistosome population., *International journal for parasitology* **46**, 417–424 (2016).

733 60. G. Mouahid, M. A. Idris, O. Verneau, A. Théron, M. M. A. Shaban, H. Moné, A new chronotype of
734 \emphSchistosoma mansoni: adaptive significance., *Trop Med Int Health* **17**, 727–732 (2012).

735 61. R. K. Assaré, R. N. N'Tamon, L. G. Bellai, J. A. Koffi, T.-B. I. Mathieu, M. Ouattara, E. Hürlimann, J. T.
736 Coulibaly, S. Diabaté, E. K. N'Goran, J. Utzinger, Characteristics of persistent hotspots of Schistosoma mansoni in
737 western Côte d'Ivoire., *Parasites & vectors* **13**, 337 (2020).

738 62. K. M. Bonner, C. J. Bayne, M. K. Larson, M. S. Blouin, Effects of Cu/Zn superoxide dismutase (SOD1)
739 genotype and genetic background on growth, reproduction and defense in *Biomphalaria glabrata*., *PLoS Negl Trop*
740 *Dis* **6**, e1701 (2012).

741 63. F. A. Lewis, M. A. Stirewalt, C. P. Souza, G. Gazzinelli, Large-scale laboratory maintenance of *Schistosoma*
742 *mansoni*, with observations on three schistosome/snail host combinations., *J Parasitol* **72**, 813–829 (1986).

743 64. D. Cioli, L. Pica-Mattoccia, R. Moroni, Schistosoma mansoni: hycanthone/oxamniquine resistance is controlled
744 by a single autosomal recessive gene., *Experimental parasitology* **75**, 425–432 (1992).

745 65. R. H. Duvall, W. B. DeWitt, An improved perfusion technique for recovering adult schistosomes from
746 laboratory animals., *The American journal of tropical medicine and hygiene* **16**, 483–486 (1967).

747 66. W. Le Clec'h, R. Diaz, F. D. Chevalier, M. McDew-White, T. J. C. Anderson, Striking differences in virulence,
748 transmission and sporocyst growth dynamics between two schistosome populations., *Parasites & vectors* **12**, 485
749 (2019).

750 67. H. Li, R. Durbin, Fast and accurate short read alignment with Burrows-Wheeler transform., *Bioinformatics*
751 *(Oxford, England)* **25**, 1754–1760 (2009).

752 68. H. Li, B. Handsaker, A. Wysoker, T. Fennell, J. Ruan, N. Homer, G. Marth, G. Abecasis, R. Durbin, 1000
753 Genome Project Data Processing Subgroup, The sequence Alignment/Map format and SAMtools., *Bioinformatics*
754 *(Oxford, England)* **25**, 2078–2079 (2009).

755 69. M. A. DePristo, E. Banks, R. Poplin, K. V. Garimella, J. R. Maguire, C. Hartl, A. A. Philippakis, G. del Angel,
756 M. A. Rivas, M. Hanna, A. McKenna, T. J. Fennell, A. M. Kernytsky, A. Y. Sivachenko, K. Cibulskis, S. B.
757 Gabriel, D. Altshuler, M. J. Daly, A framework for variation discovery and genotyping using next-generation DNA
758 sequencing data., *Nature genetics* **43**, 491–498 (2011).

bioRxiv preprint doi: https://doi.org/10.1101/2021.06.09.447779; this version posted June 10, 2021. The copyright holder for this preprint (which was not certified by peer review) is the author/funder, who has granted bioRxiv a license to display the preprint in perpetuity. It is made available under aCC-BY-NC 4.0 International license.

759 70. A. McKenna, M. Hanna, E. Banks, A. Sivachenko, K. Cibulskis, A. Kernytsky, K. Garimella, D. Altshuler, S.
760 Gabriel, M. Daly, M. A. DePristo, The genome analysis toolkit: a MapReduce framework for analyzing next-
761 generation DNA sequencing data., *Genome research* **20**, 1297–1303 (2010).

762 71. J. Köster, S. Rahmann, Snakemake-a scalable bioinformatics workflow engine., *Bioinformatics (Oxford,*
763 *England)* **34**, 3600 (2018).

764 72. F. D. Chevalier, W. Le Clec'h, A. C. Alves de Mattos, P. T. LoVerde, T. J. C. Anderson, Real-time PCR for
765 sexing Schistosoma mansoni cercariae., *Mol Biochem Parasitol* **205**, 35–38 (2016).

766 73. A. M. Emery, F. E. Allan, M. E. Rabone, D. Rollinson, Schistosomiasis collection at NHM (SCAN)., *Parasites*
767 *& vectors* **5**, 185 (2012).

768 74. R Core Team, R: A language and environment for statistical computing, *R Foundation for Statistical Computing*
769 *- Vienna, Austria* (2018).

770 75. M. O.J., PerlPrimer: cross-platform, graphical primer design for standard, bisulphite and real-time PCR.,
771 *Bioinformatics* **20**, 2471–2 (2004).

772 76. G. Krautz-Peterson, R. Bhardwaj, Z. Faghiri, C. A. Tararam, P. J. Skelly, RNA interference in schistosomes:
773 machinery and methodology., *Parasitology* **137**, 485–495 (2010).

774 77. R. Bhardwaj, G. Krautz-Peterson, P. J. Skelly, Using RNA interference in schistosoma mansoni., *Methods in*
775 *molecular biology (Clifton, N.J.)* **764**, 223–239 (2011).

776 78. X. Rao, X. Huang, Z. Zhou, X. Lin, An improvement of the 2ˆ(-delta delta CT) method for quantitative real-time
777 polymerase chain reaction data analysis., *Biostatistics, bioinformatics and biomathematics* **3**, 71–85 (2013).

778 79. G. Krautz-Peterson, R. Bhardwaj, Z. Faghiri, C. A. Tararam, P. J. Skelly, RNA interference in schistosomes:
779 machinery and methodology., *Parasitology* **137**, 485–495 (2010).

780 80. W. Le Clec'h, R. Diaz, F. D. Chevalier, M. McDew-White, T. J. C. Anderson, Striking differences in virulence,
781 transmission and sporocyst growth dynamics between two schistosome populations., *Parasites & vectors* **12**, 485
782 (2019).

783

784 **Acknowledgments:** We thank the Vivarium of the Southwest National Primate Research Center (SNPRC)
785 for providing rodent care. This research was supported by a Cowles fellowship (WLC) from Texas
786 Biomedical Research Institute (13-1328.021), and NIH R01AI133749 (TJCA) and was conducted in
787 facilities constructed with support from Research Facilities Improvement Program grant C06 RR013556
788 from the National Center for Research Resources. SNPRC research at Texas Biomedical Research Institute
789 is supported by grant P51 OD011133 from the 570 Office of Research Infrastructure Programs, NIH.
790 Miracidia samples for sequence analysis were provided by Schistosomiasis Collection at the Natural
791 History Museum (SCAN) funded by the Wellcome Trust (grant 104958/Z/14/Z) and curated Muriel

bioRxiv preprint doi: https://doi.org/10.1101/2021.06.09.447779; this version posted June 10, 2021. The copyright holder for this preprint (which was not certified by peer review) is the author/funder, who has granted bioRxiv a license to display the preprint in perpetuity. It is made available under aCC-BY-NC 4.0 International license.

792 Rabone. We thank Dr Oumar T. Diaw and Moumoudane M. Seye (Institut Sénégalais de Recherches
793 Agricoles, Senegal) for the collections in Senegal (EU-CONTRAST project); Dr Anouk Gouvras (Global
794 Schistosomiasis Alliance (GSA)), Mariama Lamine and the Re´seau International Schistosomiases
795 Environnemental Aménagement et Lutte (RISEAL) team (Niger) for the collections in Niger; Dr Anouk
796 Gouvras (GSA) and the National Institute for Medical Research (NIMR, Mwanza Tanzania) team Dr Teckla
797 Angelo, Honest Nagai, Boniface Emmanuel, John Igogote, Sarah Buddenborg and Reuben Jonathan for the
798 collections in Tanzania as part of the Schistosomiasis Consortium for Operational Research and Evaluation
799 (SCORE) project (https://score.uga.edu).

800 **Funding:**

801 National Institutes of Health grant 1R01AI123434 (TJCA, PTL)
802 National Institutes of Health grant 1R01AI133749 (TJCA)
803 National Institutes of Health grant NIH R01AI145871 (JSM)
804 Ministry of Health in Oman, the Sultan Qaboos University (grant no. IG/ MED/MICR/00/01)
805 French Ministry of Foreign Affairs (French Embassy in Oman) (grants nos. 402419B, 402415K
806 and 339660F)
807 CNRS- Sciences de la Vie (grants no. 01N92/0745/1 and 02N60/1340)
808 CNRS-Direction des Relations internationales (grants no. 01N92/0745 and 02N60/1340)
809 PICS-CNRS no. 06249: FRANC-INCENSE

810 **Author contributions:**

811 Conceptualization: WLC, PTL, TJCA
812 Methodology: WLC, FDC, PTL, JM
813 Investigation: WLC, FDC, ACM, AS, RD, JM
814 Visualization: WLC, FDC
815 Field samples: HM, GM, MI, KAM, SAY
816 Funding acquisition: TJCA, PTL, JM, HM, GM

bioRxiv preprint doi: https://doi.org/10.1101/2021.06.09.447779; this version posted June 10, 2021. The copyright holder for this preprint (which was not certified by peer review) is the author/funder, who has granted bioRxiv a license to display the preprint in perpetuity. It is made available under aCC-BY-NC 4.0 International license.

817 Project administration: TJCA, PTL

818 Supervision: TJCA, WLC, FDC, PTL, JM

819 Writing – original draft: TJCA, WLC, FDC

820 Writing – review & editing: TJCA, WLC, FDC, PTL, JM, HM, GM

821 **Competing interests:** Authors declare that they have no competing interests.

822 **Data and materials availability:**

823 Sequence data is available from: PRJNA699326, PRJNA701978, PRJNA704646

824 Sequence data from field collected *S. mansoni* is available from: PRJNA439266, PRJNA560070,
825 PRJNA560069, PRJNAXXXXXX

826 Code is available from: https://github.com/fdchevalier/PZQ-R_DNA, https://github.com/fdchevalier/PZQ-
827 R_RNA, https://github.com/fdchevalier/PZQ-R_field

828

bioRxiv preprint doi: https://doi.org/10.1101/2021.06.09.447779; this version posted June 10, 2021. The copyright holder for this preprint (which was not certified by peer review) is the author/funder, who has granted bioRxiv a license to display the preprint in perpetuity. It is made available under aCC-BY-NC 4.0 International license.

**File S1.**

# EXPANDED MATERIALS AND METHODS

## Study design

This study was designed to determine the genetic basis of PZQ-R, and was stimulated by the initial observation that a laboratory *S. mansoni* population generated through selection with PZQ contained both PZQ-S and PZQ-R individuals. The project had 6 stages:(i) QTL location. We conducted a genome-wide association study (GWAS). This involved measuring the PZQ-response of individual worms, pooling those showing high levels of resistance and low levels of resistance, sequencing the pools to high read depth, and then identifying the genome regions showing significant differences in allele frequencies between high and low resistance parasites. (ii) Fine mapping of candidate genes. We identified potential candidate genes in these QTL regions, through examination of gene annotations, and exclusion of genes that are not expressed in adults. We also determined whether the loci determining PZQ-R are inherited in a recessive, dominant or co-dominant manner (iii) Marker assisted purification of PZQ-S and PZQ-R parasites. To separate PZQ-R and PZQ-S parasites into "pure" populations, we genotyped larval parasites for genetic markers in the QTL regions and infected rodents with genotypes associated with PZQ-R or PZQ-S. To verify that this approach worked, we then measured the $IC_{50}$ for each of the purified populations. (iv) Characterization of purified SmLE-PZQ-ER and SmLE-PZQ-ES populations. Separation of SmLE-PZQ-ES and SmLE-PZQ-ER parasite populations allowed us to characterize these in more detail. Specifically, we measured expression in juvenile and adult worms of both sexes in both SmLE-PZQ-ES and SmLE-PZQ-ER parasites. We also quantified parasite fitness traits. (v) Functional analysis. We used RNAi and chemical manipulation approaches to modulate activity of candidate genes and determine the impact of PZQ-resistance. We also used transient expression of candidate genes in cultured mammalian cells, to determine the impact of particular SNPs on response to PZQ-exposure. (vi) Survey of PZQ-resistance variants in field collected parasites. Having determined the gene underlying PZQ-R in laboratory parasites, we examined sequence

bioRxiv preprint doi: https://doi.org/10.1101/2021.06.09.447779; this version posted June 10, 2021. The copyright holder for this preprint (which was not certified by peer review) is the author/funder, who has granted bioRxiv a license to display the preprint in perpetuity. It is made available under aCC-BY-NC 4.0 International license.

853 variation in this gene in a field collection of *S. mansoni* parasites collected to examine the frequency of
854 sequence variants predicted to result in PZQ-resistance.
855
856 Ethics statement
857 This study was performed in accordance with the Guide for the Care and Use of Laboratory Animals of the
858 National Institutes of Health. The protocol was approved by the Institutional Animal Care and Use
859 Committee of Texas Biomedical Research Institute (permit number: 1419-MA and 1420-MU). Details of
860 ethical permission for collection of samples from humans are described in Chevalier et al. *(51, 52)*.
861
862 **Biomphalaria glabrata *snails and* Schistosoma mansoni *parasites***
863 Uninfected inbred albino *Biomphalaria glabrata* snails (line Bg121 derived from 13-16-R1 line *(62)*) were
864 reared in 10-gallon aquaria containing aerated freshwater at 26-28 °C on a 12L-12D photocycle and fed *ad*
865 *libitum* on green leaf lettuce. All snails used in this study had a shell diameter between 8 and 10 mm. We
866 used inbred snails to minimize the impact of snail host genetic background on the parasite life history traits
867 *(66)*.
868 The SmLE schistosome (*Schistosoma mansoni*) population was originally obtained from an
869 infected patient in Belo Horizonte (Minas Gerais, Brazil) in 1965 and has since been maintained in
870 laboratory *(63)*, using *B. glabrata* NMRI, inbred Bg36 and Bg121 population as intermediate snail host and
871 Syrian golden hamsters (*Mesocricetus auratus*) as definitive hosts. The SmLE-PZQ-R schistosome
872 population was generated in Brazil by applying a single round of PZQ selection pressure on SmLE parasites
873 at both snail and rodent stages *(26)*. The SmLE-PZQ-R population has been maintained in our laboratory
874 using *B. glabrata* NMRI, Bg36 and Bg121 snail population and hamsters as the definitive host since 2014.
875
876 **Drug resistance tests:**
877 *Dose-response curves to PZQ in SmLE and SmLE-PZQ-R populations*

bioRxiv preprint doi: https://doi.org/10.1101/2021.06.09.447779; this version posted June 10, 2021. The copyright holder for this preprint (which was not certified by peer review) is the author/funder, who has granted bioRxiv a license to display the preprint in perpetuity. It is made available under aCC-BY-NC 4.0 International license.

Drug sensitivity to Praziquantel (PZQ) was initially measured using a modified protocol *(64)* in SmLE and SmLE-PZQ-R parasite populations. Ten adult males, recovered by perfusion from infected hamsters (t+ 45 days post-infection) *(65)* from SmLE or SmLE-PZQ-R population were placed into each well of a 24-well microplate containing 1 mL of High glucose DMEM supplemented with 15% heat-inactivated fetal bovine serum, 100 U/mL penicillin and 100µg/mL streptomycin (DMEM complete media). We performed control and experimental groups in triplicate (*N*=240 worms/parasite populations). We exposed adult worms to PZQ (0.1 µg/mL, 0.3 µg/mL, 0.9 µg/mL, 2.7 µg/mL, 8.1 µg/mL, 24.3 µg/mL and 72.9 µg/mL) for 24h. Worms were then washed three times in drug-free medium and incubated (37ºC, 5% $CO_2$) for 2 days. Control groups were exposed only to the drug diluent dimethyl sulfoxide (DMSO). The parasites were observed daily under a stereomicroscope for the 5 days of the experiment and the number of dead worms visually scored. Worms were defined as "dead" if they showed no movements and became opaque. We scored PZQ-resistance as a binary trait: parasites that recovered were classed as resistant, while parasites that failed to recover were classed as sensitive.

*Metabolic assessment of worm viability using L-lactate assay*

We adapted a method for metabolic assessment of worm viability using L-lactate assay *(44)*. Briefly, adult male SmLE-PZQ-R worms recovered from infected hamsters were placed individually in 96-well plates containing 100 µm mesh filter insert (Millipore) in 250µL DMEM complete media, and allowed to adapt for 24 h. We added PZQ (24.3 µg/mL in DMEM complete media) for the PZQ treated group, while controls were treated with the same volume of drug diluent DMSO. We also added a heat-killed worm control group: adult male worms were placed into a microfuge tube containing distilled water and heated in a dry bath (80ºC, 15 min), and then plated in 96-well plate with 100 µm mesh insert. Drug resistance test was conducted as described above (see *Dose-response curves to PZQ in SmLE and SmLE-PZQ-R populations*). At 48h post-treatment, the supernatant (125 µL) was collected from each well and immediately stored at -80 °C until processing.

bioRxiv preprint doi: https://doi.org/10.1101/2021.06.09.447779; this version posted June 10, 2021. The copyright holder for this preprint (which was not certified by peer review) is the author/funder, who has granted bioRxiv a license to display the preprint in perpetuity. It is made available under aCC-BY-NC 4.0 International license.

We measured lactate levels in the supernatants of *in vitro* treated adult male worms with a colorimetric L-lactate assay kit (Sigma) using 96-well, optical clear-bottom plates (Corning) following the manufacturer's specifications, with minor modifications. Briefly, 5 µL of supernatant were diluted into 20 µL of dd$H_2O$ to fit within the linear range of the assay. We then combine 24 µL of the assay buffer to 1 µL of diluted supernatant (1/5 dilution) in each test well. and added 25 µL of the lactate reaction mix (24 µL of the assay buffer, 0.5 µL of enzyme mix and 0.5 µL of lactate assay probe - $V_{total}$= 50 µL/well). We also made a lactate standard curve to allow accurate lactate quantification in worm supernatants. After 45 min of incubation in the dark at room temperature, the plate was read by a spectrophotometer (Molecular Devices) at 570 nm. Lactate quantities in worm supernatant were assessed following the manufacturer's instruction, taking in account our dilution factor. All measurement series included a DMEM complete media control to determine the background lactate level, which was then subtracted from the lactate quantity of the respective measurements.

## Genome wide association analysis and QTL mapping

*Schistosome infections*

Eggs were collected from livers of hamster infected with SmLE-PZQ-R and hatched under light for 30 min in freshwater to obtain miracidia *(66)*. We then exposed one thousand Bg121 snails to five miracidia/snail. After 30 days, snails were individually exposed to light in 24-well plates to shed cercariae. Eight hamsters were exposed to 840 cercariae (4 cercariae/snail) from a batch of 210 shedding snails. We euthanized hamsters after 45 days to collect adult worms.

*Phenotypic selection*

Adult SmLE-PZQ-R worms were collected, separated by sex and males were plated individually in 96-well plates (60 worms per plate) containing 100uM mesh filter insert (Millipore) in 250 µL of DMEM complete media and treated with a dose of 24.3 µg/mL PZQ as describe above (i.e. *Metabolic assessment of worms viability using L-lactate assay*). A group of 12 worms were treated with the same volume of drug diluent

bioRxiv preprint doi: https://doi.org/10.1101/2021.06.09.447779; this version posted June 10, 2021. The copyright holder for this preprint (which was not certified by peer review) is the author/funder, who has granted bioRxiv a license to display the preprint in perpetuity. It is made available under aCC-BY-NC 4.0 International license.

DMSO. This GWAS experiment was done twice independently. A total of 590 and 691 adult male worms were collected, cultured *in vitro* and exposed to PZQ for the two experiments respectively.

Worm media supernatants (125 µL) were collected in 96-well PCR plates after 24h in culture (to assess the viability of the worms before PZQ treatment – adult male worms should release ≥ 40 nmol/h of lactate in supernatant) and 48h post-treatment (to assess their viability after PZQ treatment). Plates containing supernatant were immediately stored at -80 °C until processing. Lactate levels in supernatants were quantified as described above (see *Metabolic assessment of worm viability using L-lactate assay*). We phenotype the worms and categorize them into two groups: i) Recovered worms (i.e. releasing ≥ 40 nmol/h of lactate in supernatant) and ii) Susceptible worms (i.e. releasing less 40 nmol/h of lactate in supernatant). Among these two groups, we took the 20% of the treated worms releasing in their media the highest amount of lactate (average L-lactate production ± SD: Experiment 1 = 61.44 nmol/h ± 13.16 / Experiment 2 = 56.38 nmol/h ± 10.82) and the 20% of the treated worms releasing the lowest amount of lactate (average L-lactate production ± SD: Experiment 1 = 28.61 nmol/h ± 5.32 / Experiment 2 = 23.04 nmol/h ± 4.14), 48h post PZQ treatment respectively.

*DNA extraction and library preparation*

We sequenced whole genomes of the two pools of recovered (i.e. resistant to PZQ, Experiment 1: 116 worms / Experiment 2: 137 worms) and susceptible worms (Experiment 1: 116 worms / Experiment 2: 137 worms). We then estimated allele frequencies in each pool to identify genome regions showing high differentiation.

a. ***gDNA extraction:*** We extracted gDNA from pools of worms using the Blood and Tissue kit (Qiagen). We homogenized worms in DNA extraction kit lysis buffer using sterile micro pestles., incubated homogenates (56 °C, 2 hour) and recovered gDNA in 200 µL of elution buffer. We quantified the worm gDNA recovered using the Qubit dsDNA HS Assay Kit (Invitrogen).

*b.* ***Whole genome library preparation and sequencing:*** We prepared whole genome libraries from pools of worm gDNA in triplicate using the KAPA HyperPlus kit (KAPA Biosystems) according to

bioRxiv preprint doi: https://doi.org/10.1101/2021.06.09.447779; this version posted June 10, 2021. The copyright holder for this preprint (which was not certified by peer review) is the author/funder, who has granted bioRxiv a license to display the preprint in perpetuity. It is made available under aCC-BY-NC 4.0 International license.

the manufacturer's protocol. For each library, we sheared 100 ng of gDNA by adaptive focused acoustics (Duty factor: 10%; Peak Incident Power: 175; Cycles per Burst: 200; Duration: 180 seconds) in AFA tubes (Covaris S220 with SonoLab software version 7 (Covaris, Inc., USA)) to recover fragmented DNA (150-200 bp). Library indexing was done using KAPA Dual Adapters at 15 µM for 1h. We used 6 PCR cycles for post-ligation library amplification. We performed size selection on the indexed-amplified libraries using KAPA Pure bead (0.7x first upper size cut; 0.9x second lower size cut). We quantified libraries by qPCR using KAPA library quantification kit (KAPA Biosystems) and their respective fragment size distribution was assessed by TapeStation (Agilent). We sequenced the libraries on a HiSeq X sequencer (Illumina) using 150 bp pair-end reads. Raw sequence data are available at the NCBI Sequence Read Archive (PRJNA699326).

*Bioinformatic analysis*

Jupyter notebook and scripts used for processing the sequencing data and identifying the QTL are available on Github (https://github.com/fdchevalier/PZQ-R_DNA).

a. ***Sequence analysis and variant calling:*** We aligned the sequencing data against the *S. mansoni* reference genome (schistosoma_mansoni.PRJEA36577.WBPS14) using BWA (v0.7.17) *(67)* and SAMtools (v1.10) *(68)*. We used GATK (v4.1.8.1) *(69, 70)* to mark PCR duplicates and recalibrate base scores. We used the HaplotypeCaller module of GATK to call variants (SNP/indel) and the GenotypeGVCFs module to perform a joint genotyping on each chromosome or unassembled scaffolds. We merged VCF files using the MergeVcfs module. All these steps were automatized using Snakemake (v5.14.0) *(71)*.

b. ***QTL identification:*** We expect the genome region underlying resistance to be enriched in variants from high lactate producing worms. To evaluate statistical evidence for such enrichment, we examined the difference in allele frequencies between low and high lactate parasites across the genome by calculating a *Z*-score at each bi-allelic site. To minimize bias, we weighed *Z*-scores by including the number of worms in each treatment and the difference in the total read depth across

bioRxiv preprint doi: https://doi.org/10.1101/2021.06.09.447779; this version posted June 10, 2021. The copyright holder for this preprint (which was not certified by peer review) is the author/funder, who has granted bioRxiv a license to display the preprint in perpetuity. It is made available under aCC-BY-NC 4.0 International license.

the triplicated libraries of each treatment at the given variant. We calculated $Z$-scores for each biological replicate as follows:

$$Z = \frac{p_1 - p_2}{\sqrt{p_0(1-p_0)\left(\frac{1}{x.n_1} + \frac{1}{x.n_2} + \frac{1}{d_1} + \frac{1}{d_2}\right)}}$$

where $p1$ and $p2$ are the estimated allele frequencies in the low and high lactate parasites pools, respectively; $p0$ is the allele frequency under the null hypothesis H0: $p1 = p2$ estimated from the average of $p1$ and $p2$; $n1$ and $n2$ are the number of worms in the low and high lactate parasites pools, respectively, factor $x$ for each $n$ reflecting the ploidy state ($x$=2); and $d1$ and $d2$ are the sequencing depths for the low and high lactate parasite pools, respectively.

We combined $Z$-scores generated from each biological replicate as follows:

$$Z_c = \frac{Z_1 + Z_2}{\sqrt{2}}$$

where $Z_1$ and $Z_2$ were $Z$-scores from replicate 1 and 2, respectively. The p-values were obtained by comparing the negative absolute value of $Z$-scores to the standard normal distribution. To determine the significant threshold, Bonferroni correction was calculated with $\alpha = 0.05$. These analyses are available in the Jupyter notebook and associated scripts (https://github.com/fdchevalier/PZQ-R_DNA).

**Relationship between worm genotype at Chr 2 and 3 and PZQ-R phenotype**

To validate the impact of worm genotypes on its PZQ resistance phenotypes and determine whether PZQ-R shows recessive, dominant or codominant inheritance, we determined the PZQ-R phenotype of individual worms, which were then genotyped for markers at the peak of the QTLs located.

*Measuring PZQ-R in individual worms*

bioRxiv preprint doi: https://doi.org/10.1101/2021.06.09.447779; this version posted June 10, 2021. The copyright holder for this preprint (which was not certified by peer review) is the author/funder, who has granted bioRxiv a license to display the preprint in perpetuity. It is made available under aCC-BY-NC 4.0 International license.

We collected 120 SmLE-PZQ-R adult male worms, plated them individually in 96-well plates containing a mesh filter insert, cultured them *in vitro*, treated them with PZQ (24.3 µg/mL) and collected media supernatants before (after 24h in culture) and 48h post-treatment, and used L-lactate assays to determine PZQ-R status (see *Phenotypic selection*). We extracted gDNA from each worm individually. Briefly, we transferred worms into 96-well PCR plates, added 100 µL of 6% Chelex® solution containing 1% Proteinase K (20 mg/mL), incubated for 2h at 56 °C and 8 min at 100 °C, and transferred the supernatant containing worm gDNA into fresh labeled 96-well plates.

*PCR-RFLP conditions for Chr.2 and Chr.3 loci*

We used PCR-RFLP to genotype single worms at loci marking QTL peaks on chr. 2 (C>A, chr SMV7_2: 1072148) and chr. 3 (T>C, chr SMV7_3: 741987). Primers were designed using PerlPrimer v1.21.1 *(75)* (Table S4). We digested PCR amplicons for chr. 2 with BslI (NEB) and chr. 3 with Mse1 (NEB), and visualized digested PCR amplicons by 2% agarose gel electrophoresis.

*Quantitative PCR validation of copy number variation (CNV) in single worms*

We genotyped each individual worm for a deletion identified on chr. 3 at position 1220683- 1220861 bp using a custom quantitative PCR assay. This was done to examine the association between deletion of this genomic region and PZQ resistant genotype. We quantified the copy number in this region relative to a single copy gene from *S. mansoni* (α-tubulin 2, LeClech2019). The CNV genotype for each parasite corresponds to the ratio of the CNV copy number and the α-tubulin 2 gene copy number: 0=complete deletion, 0.5=one copy, 1=two copies. Methods and primers are described in Table S4. We then compared individual worm phenotypes for each of the three CNV genotypes (0, 1 or 2 copies) to determine the association between CNV and PZQ response.

**Marker assisted selection of resistant and susceptible parasite populations**

*Selection of SmLE-PZQ-ER and SmLE-PZQ-ES populations*

bioRxiv preprint doi: https://doi.org/10.1101/2021.06.09.447779; this version posted June 10, 2021. The copyright holder for this preprint (which was not certified by peer review) is the author/funder, who has granted bioRxiv a license to display the preprint in perpetuity. It is made available under aCC-BY-NC 4.0 International license.

We separated the polymorphic SmLE-PZQ-R schistosome population based on chr. 3 QTL genotype using the PCR-RFLP as described. We exposed 960 inbred *B. glabrata* Bg121 snails to one miracidium SmLE-PZQ-R *(66)*. At four weeks post-exposure, we identified infected snail (*N*=272), and collected cercariae from individual snails. We extracted cercarial DNA using 6%Chelex *(66)*), and genotyped each parasite for chr. 3 locus using our PCR-RFLP (Homozygous R/R: n=89 – 36%; Homozygous S/S: n=39 – 16%; Heterozygous R/S: n=117 – 49%) and determine their gender by PCR *(72)*. We selected 32 R/R parasites (homozygous for the $Sm.TRPM_{PZQ}$ resistant-associated allele) and 32 S/S genotypes (i.e. homozygous for the $Sm.TRPM_{PZQ}$ sensitive-associated allele). For both R/R and S/S we used 13 males and 19 females. We exposed 5 hamsters to 800 cercariae of 32 R/R genotypes parasites and 5 hamsters to 800 cercariae 32 S/S genotyped parasites. This single generation marker assisted selection procedure generates two subpopulations: SmLE-PZQ-ER is expected to be enriched for parasites with R/R genotype and to show strong PZQ-R, while SmLE-PZQ-ES is enriched for S/S genotypes and is expected to be highly sensitive to PZQ).

*PZQ $IC_{50}$ with SmLE-PZQ-ER and SmLE-PZQ-ES*

Forty-five days after exposure to cercariae, we euthanized and perfused hamsters to recover adult schistosome worms for each of the two subpopulations (SmLE-PZQ-ER and SmLE-PZQ-ES). We separated worms by sex and we set adult males in 96-well plates containing 100 µm mesh filter insert (Millipore) and cultured in 250 µL DMEM complete media as described.

We determined PZQ dose-response for both SmLE-PZQ-ER and SmLE-PZQ-ES population. We exposed individual worms (*N*=60/population/treatment) to PZQ (0.1 µg/mL, 0.3 µg/mL, 0.9 µg/mL, 2.7 µg/mL, 8.1 µg/mL, 24.3 µg/mL and 72.9 µg/mL) or drug diluent (DMSO control). Worm media supernatants (125µL) were collected in 96-well PCR plates before treatment (after 24h in culture) and 48h post-treatment. We quantified lactate levels in supernatants described and we assess variation in lactate production for each individual worm.

bioRxiv preprint doi: https://doi.org/10.1101/2021.06.09.447779; this version posted June 10, 2021. The copyright holder for this preprint (which was not certified by peer review) is the author/funder, who has granted bioRxiv a license to display the preprint in perpetuity. It is made available under aCC-BY-NC 4.0 International license.

*gDNA extraction and library preparation*

SmLE-PZQ-ER and SmLE-PZQ-ES parasite populations were maintained in our laboratory. We recovered the F1 worms from each populations and extract gDNA from pools of adult males and females separately as described above. We prepared whole genome libraries from these pools in triplicate using the KAPA HyperPlus kit (KAPA Biosystems) as described (see *Whole genome library preparation and sequencing*). We sequenced the libraries on a HiSeq X sequencer (Illumina) using 150 bp paired-end reads. Sequence data are available at the NCBI Sequence Read Archive (accession numbers PRJNA701978).

*Bioinformatic analysis*

The analysis was identical to the GWAS and QTL mapping analysis. This can be replicated with the Jupyter notebook and associated scripts (https://github.com/fdchevalier/PZQ-R_DNA).

## Transcriptomic analysis of resistant and susceptible schistosome worms to PZQ at juvenile (28 days) and adult (45 days) stages

*Sample collection*

Juvenile and adult *S. mansoni* SmLE-PZQ-ER and SmLE-PZQ-ES worms were recovered by perfusion from hamsters at 28 days (juveniles) or 45 days (adults) post-infection. Worms from each population were placed in DMEM complete media, separated by sex, and aliquoted in sterile RNAse free microtubes which were immediately snap-frozen in liquid nitrogen and stored at -80 °C until RNA extractions. For each subpopulation, (SmLE-PZQ-ER or SmLE-PZQ-ES), we collected 3 biological replicates of 30 males and 3 replicates of 30 females for the 28d juvenile worms and 3 biological replicates of 30 males and 3 replicates of 60 females for the 45d adult worms.

*RNA extraction and RNAseq library preparation*

***a. RNA extraction***

bioRxiv preprint doi: https://doi.org/10.1101/2021.06.09.447779; this version posted June 10, 2021. The copyright holder for this preprint (which was not certified by peer review) is the author/funder, who has granted bioRxiv a license to display the preprint in perpetuity. It is made available under aCC-BY-NC 4.0 International license.

We extracted total RNA from all the *S. mansoni* adult and juvenile worms collected using the RNeasy Mini kit (Qiagen). Samples were randomized prior to RNA extraction to minimize batch effects. We homogenized worms in 600 µL RNA lysis buffer (RTL buffer, Qiagen) using sterile micro pestles, followed by passing the worm lysate 10 times through a sterile needle (23 gauge). We recovered total RNA in 25 µL elution buffer. We quantified the RNA recovered using the Qubit RNA Assay Kit (Invitrogen) and assessed the RNA integrity by TapeStation (Agilent - RNA integrity numbers of ~8.5–10 for all the samples).

***b. RNAseq library preparation***

We prepared RNAseq libraries using the KAPA Stranded mRNA-seq kit (KAPA Biosystems) using 500ng RNA diluted in 50uL Tris-HCl (pH 8.0) for each library. We fragmented mRNA (6 min 94ºC), indexed libraries using 3'-dTMP adapters (7µM, 1 hour at 20ºC), and used 6 PCR cycles for post-ligation library amplification. We quantified indexed libraries by qPCR (KAPA library quantification kit (KAPA Biosystems)) and assessed their fragment size distribution by TapeStation (Agilent). We sequenced the libraries on a HiSeq 4000 sequencer (Illumina) using 150 bp pair-end reads, pooling 12 RNAseq libraries/lane. Raw sequence data are available at the NCBI Sequence Read Archive under accession numbers PRJNA704646.

***c. Bioinformatic analysis.***

To identify differentially expressed genes between the different groups, we aligned the sequencing data against the *S. mansoni* reference genome (schistosoma_mansoni.PRJEA36577.WBPS14) using STAR (v2.7.3a) (ref). We quantified gene and isoform abundances by computing transcripts per million values using RSEM (v1.3.3) (ref). We compared these abundances between groups (ES/ER, males/females, juveniles/adults) using the R package EBSeq (v1.24.0) (ref). Jupyter notebooks and associated scripts are available on Github (https://github.com/fdchevalier/PZQ-R_RNA).

**Manipulation of *Sm.TRPM$_{PZQ}$* channel expression or function:**

*RNA interference*

bioRxiv preprint doi: https://doi.org/10.1101/2021.06.09.447779; this version posted June 10, 2021. The copyright holder for this preprint (which was not certified by peer review) is the author/funder, who has granted bioRxiv a license to display the preprint in perpetuity. It is made available under aCC-BY-NC 4.0 International license.

We used RNA interference to knock down the expression of Smp_246790 gene in order to functionally validate the implication of *Sm.TRPM*$_{PZQ}$ on schistosome PZQ resistance. SmLE-PZQ-R adult male worms were freshly recovered from infected hamsters and placed in 24-well plates for in vitro culture (10 adult male worms/well).

***a. siRNA treatment on* S. mansoni *adult male worms***

Small inhibitory RNAs (siRNAs) targeting specific schistosome genes were designed using the on-line IDT RNAi Design Tool (https://www.idtdna.com/Scitools/Applications/RNAi/RNAi.aspx) (Table S2) and synthesized commercially by Integrated DNA Technologies (IDT, Coralville, IA). To deliver the siRNAs, we electroporated schistosome parasites (10 adults/group – each group done in triplicate) in 100 µL RPMI medium containing 2.5 µg siRNA or the equivalent volume of dd$H_2O$ (no siRNA control), in a 4 mm cuvette by applying a square wave with a single 20 ms impulse, at 125 V and at room temperature (Gene Pulser Xcell Total System (BioRad)) *(76, 77)*. Parasites were then transferred to 1 mL of complete DMEM media in 24-well plates. After overnight culture, medium was replaced with fresh DMEM complete media. We measured gene expression by quantitative real-time PCR (RT-qPCR) 2 days after siRNA treatment.

***b. dsRNA treatment on* S. mansoni *adult male worms***

We synthetized double-stranded RNA according to Wang et al., 2020 (Table S2). For dsRNA treatment, 10 adult male worms/group (each group done in triplicate) were cultured in 1 mL DMEM complete media and treated with 90 ug dsRNA at day 0, day 1 and day 2. Media was changed every 24h and fresh dsRNA was added. On day 3, we harvested worms and measured gene expression by quantitative real-time PCR (RT-qPCR).

***c. RNA extraction and gene expression analysis by RT-qPCR***

We extracted total RNA from parasites (*N*=10 worms/sample) using the RNeasy Mini kit (Qiagen) (see *RNA extraction*). Complementary DNA (cDNA) was generated from extracted RNA (500 ng - 1 µg) using SuperScript-III and Oligo-dT primers (ThermoFisher). Relative quantification of genes of interest was performed in duplicate by qPCR analysis using QuantStudio 5 System (Applied Biosystems) and SYBR Green master mix (ThermoFisher), compared with a serially diluted standard of PCR products (generated

bioRxiv preprint doi: https://doi.org/10.1101/2021.06.09.447779; this version posted June 10, 2021. The copyright holder for this preprint (which was not certified by peer review) is the author/funder, who has granted bioRxiv a license to display the preprint in perpetuity. It is made available under aCC-BY-NC 4.0 International license.

from cDNA) for each of the gene tested *(66)*. Standard curves allow evaluating the efficiency of each pairs of primers, for both housekeeping and target genes using QuantStudio Design and Analysis Software. Expression was normalized to SmGAPDH housekeeping gene (Table S2) using the efficiency $E^{\Delta\Delta Ct}$ method *(78)*.

*Specific Sm.TRPM$_{PZQ}$ chemical inhibitor and activators*

We used specific chemical inhibitor and activators (Chulkov *et al.*, in prep) to manipulate the function of Sm.TRPM$_{PZQ}$ to examine the impact on PZQ-response. We placed individual SMLE-PZQ-ER and SMLE-PZQ-ES adult male worms in 96-well plates with 100 µm mesh filter insert containing DMEM complete media and cultured described above (see *Metabolic assessment of worm viability using L-lactate assay*). After 24h in culture, 20 worms from each population were treated either with a cocktail combining PZQ (1 µg/mL) and i) 50 µM of *Sm.TRPM$_{PZQ}$* blocker (MB2) or ii) 10 µM, 25 µM or 50 µM of *Sm.TRPM$_{PZQ}$* activator (MV1) respectively or iii) drug diluent (DMSO). We also set up control plates to evaluate the impact of *Sm.TRPM$_{PZQ}$* blocker or activator alone. In that case, 20 worms from each population were treated with a cocktail combining drug diluent DMSO and *Sm.TRPM$_{PZQ}$* blocker (MB2) or activator (MV1) at the same concentrations mentioned above. Worms were exposed to these drug cocktails for 24h, washed 3 times with drug-free medium, and incubated (37ºC,5% $CO_2$) for 2 days.

We collected Worm media supernatants (125µL) in 96-well PCR plates before treatment (after 24h in culture) and 48h post-treatment and Lactate levels in supernatants were quantified as described above (see *Metabolic assessment of worm viability using L-lactate assay*). We used these results to determine the impact of blockers or activators on variation in lactate production.

**_In vivo_ parasite survival after PZQ treatment**

We used 24 female Balb/C mice (purchased from Envigo at 6 weeks-old and housed in our facility for one week before use) split into two groups: one group exposed by tail immersion to SmLE-PZQ-ER (80 cercariae/mouse from 40 infected snails) and the second one to SmLE-PZQ-ES (80 cercariae/mouse from

bioRxiv preprint doi: https://doi.org/10.1101/2021.06.09.447779; this version posted June 10, 2021. The copyright holder for this preprint (which was not certified by peer review) is the author/funder, who has granted bioRxiv a license to display the preprint in perpetuity. It is made available under aCC-BY-NC 4.0 International license.

40 infected snails). Each mouse was identified by a unique tattoo ID and an ear punch for assessing treatment status (PZQ or drug diluent control). Immediately after infection, we stained the content of each infection vial with 10 µL 0.4% Trypan blue and counted all the cercarial tails/heads or complete cercariae to determine the cercarial penetration rate for each mouse. We kept infected mice in 4 cages (2 cages/parasite populations and 6 animals per cage) at 21-22º C and 39%–50% humidity and monitored them daily.

Forty days post-infection, we weighed mice and treated them by oral gavage with either 120mg/kg of PZQ (diluted in 1% DMSO + vegetable oil – Total volume given/mouse: 150 µL) or the same volume of drug diluent only (control group). To minimize batch effects, 3 mice were treated with PZQ and 3 with the drug diluent per cage for each parasite group (SmLE-PZQ-ER or SmLE-PZQ-ES). Mice were monitored daily until euthanasia and perfusion *(65)*, at day 50 post-infection. We recorded the weight of each mouse before euthanasia. After euthanasia and perfusion, we also weighted the liver and spleen of each individual. We carefully recovered worms from the portal vein, liver and intestine mesenteric venules of each mouse. Worms were separated by sex and counted.

## ***Sm.TRPM$_{PZQ}$* variants in *S. mansoni* field samples**

### *Variants identification in exome-sequenced data from natural* S. mansoni *parasites*

We utilized exome sequence data from *S. mansoni* from Africa, South America and the middle East to investigate variation in *Sm.TRPM$_{PZQ}$*. African miracidia were from the Schistosomiasis collection at the Natural History Museum (SCAN) *(73)*, Brazilian miracidia and Omani cercariae and adult worms were collected previously. We have previously described methods and generation of exome sequence from *S. mansoni* samples *(51, 52)*. Data were analyzed the same way as described in Chevalier et al. *(52)*. Code is available in Jupyter notebook and scripts associated (https://github.com/fdchevalier/PZQ-R_field).

### *Sanger re-sequencing to confirm the presence of the* Sm.TRPM$_{PZQ}$ *field variants*

bioRxiv preprint doi: https://doi.org/10.1101/2021.06.09.447779; this version posted June 10, 2021. The copyright holder for this preprint (which was not certified by peer review) is the author/funder, who has granted bioRxiv a license to display the preprint in perpetuity. It is made available under aCC-BY-NC 4.0 International license.

To confirm the presence of the variants in *Sm.TRPM$_{PZQ}$* gene from our exome-sequenced natural *S. mansoni* parasites (when read depth was <10 reads), we performed Sanger re-sequencing of eight *Sm.TRPM$_{PZQ}$* exons (i.e. exon 3, 4, 23, 25, 27, 29 and 34) where either nonsense mutations (leading to truncated protein) or non-synonymous mutation located close to the PZQ binding site *(21)* were identified. Primers and conditions are listed in Table S4.

*Sanger sequencing analysis*

We scored variants using PolyPhred software (v6.18) (Nickerson et al., 1997) which relies on Phred (v0.020425.c), Phrap (v0.990319), and Consed (v29.0) software, analyzing each exon independently. We identified single nucleotide polymorphisms using a minimum phred quality score (-q) of 25, a minimum genotype score (-score) of 70, and a reference sequence of the *Sm.TRPM$_{PZQ}$* gene from the chromosome 3 of *S. mansoni* reference genome (schistosoma_mansoni.PRJEA36577.WBPS14). Variant sites were labeled as non-reference alleles if they differed from the reference sequence. We identified insertion/deletion (indel) polymorphisms using a minimum phred quality score (-q) of 25, a minimum genotype score (-iscore) of 70. Polymorphisms were visually validated using Consed. All the sequences were submitted to GenBank (GenBank accession no KU951903-KU952091). These analyses are available in the Jupyter notebook and associated scripts (https://github.com/fdchevalier/PZQ-R_DNA).

## Statistical analysis

All statistical analyzes and graphs were performed using R software (v3.5.1) *(74)*. We used the drc package from R to analyze all our dose-response datasets using a four-parameter log-logistic function to fit curves. We used the Readqpcr and Normqpcr packages to analyze all our RT-qPCR datasets, using the *efficiency*$^{\Delta\Delta Ct}$ method. When data were not normally distributed (Shapiro test, $p < 0.05$), we compared results with non-parametric tests: Chi-square test, Kruskal-Wallis test followed by pairwise Wilcoxon-Mann-Whitney post-hoc test or a simple pairwise comparison Wilcoxon-Mann-Whitney test. When data followed a normal

bioRxiv preprint doi: https://doi.org/10.1101/2021.06.09.447779; this version posted June 10, 2021. The copyright holder for this preprint (which was not certified by peer review) is the author/funder, who has granted bioRxiv a license to display the preprint in perpetuity. It is made available under aCC-BY-NC 4.0 International license.

distribution, we used one–way ANOVA or a pairwise comparison Welsh *t*-test. The confidence interval of significance was set to 95% and *p*-values less than 0.05 were considered significant.

## SUPPLEMENTARY FIGURES

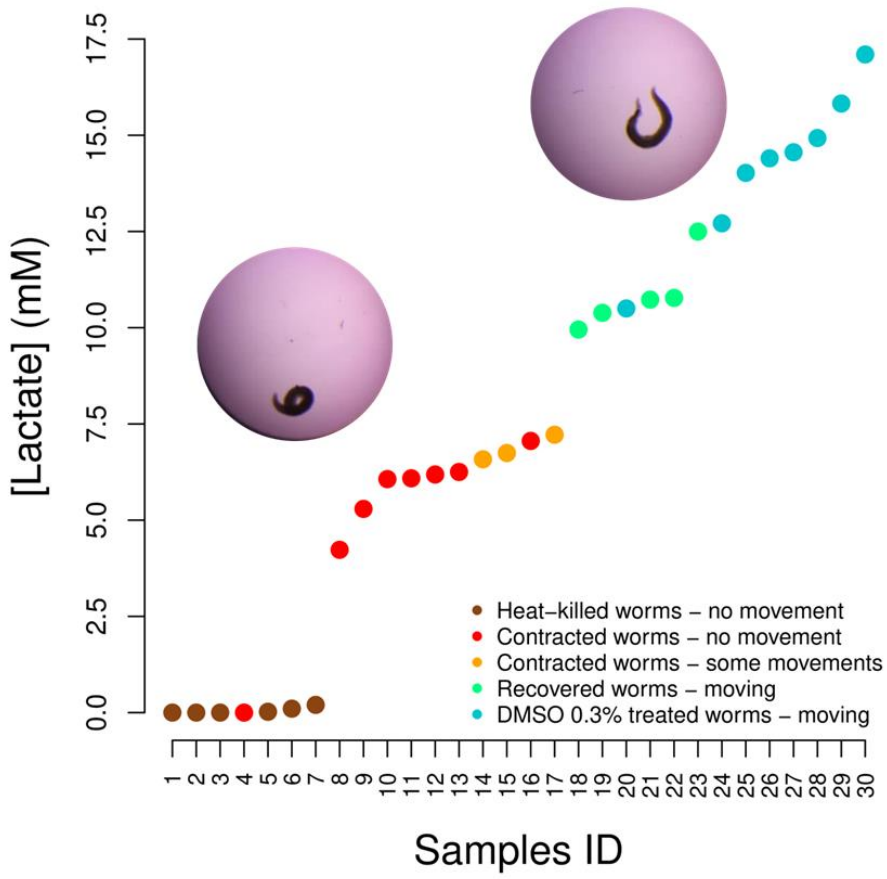
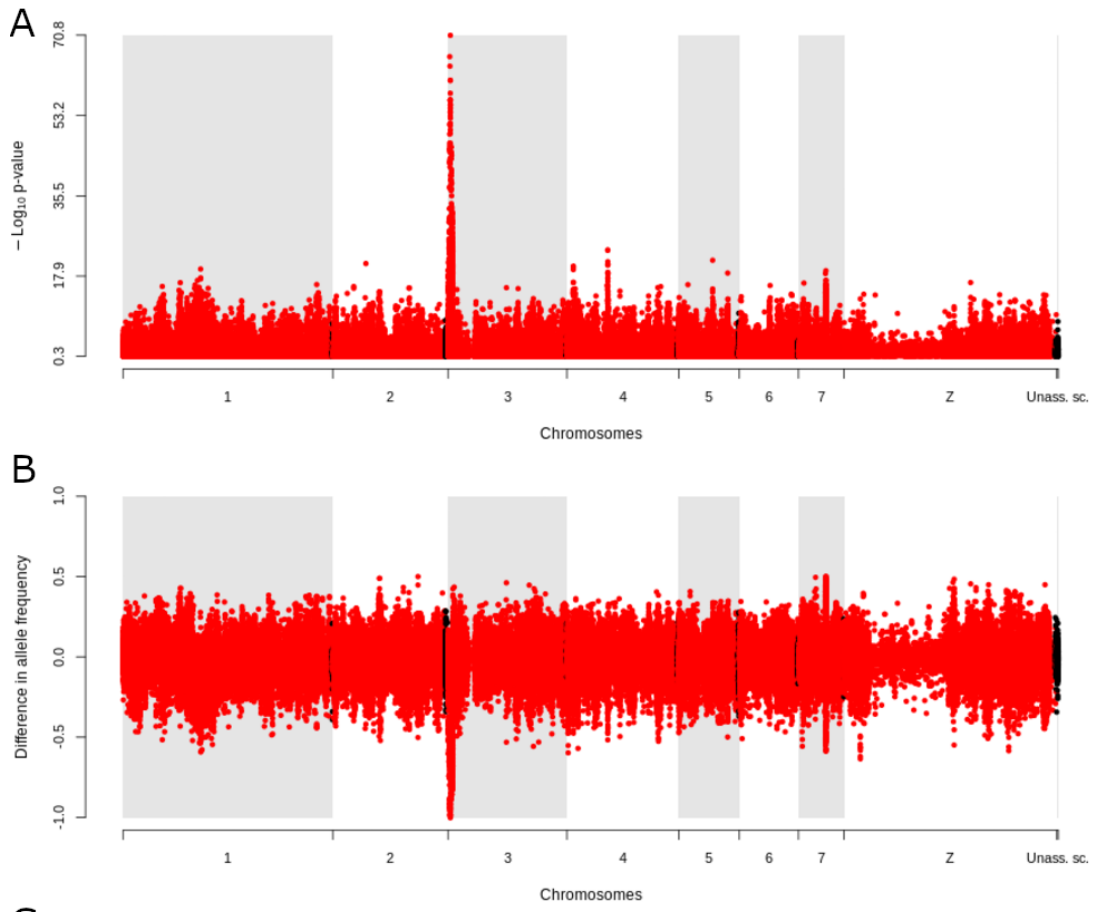



**Fig. S1. Development of a lactate assay for assaying worm recovery.** Validation of the L-lactate assay for single male worms and correlation with their microscopic appearance and ability to regain movement after PZQ treatment (24.3 µg/mL). PZQ-S worms (contracted), that remain contracted after PZQ treatment produce significantly less amount of lactate released in the media compared to PZQ-R (recovered and motile) worms (Wilcoxon test, p = 0.0015; *N* = 30 worms).

bioRxiv preprint doi: https://doi.org/10.1101/2021.06.09.447779; this version posted June 10, 2021. The copyright holder for this preprint (which was not certified by peer review) is the author/funder, who has granted bioRxiv a license to display the preprint in perpetuity. It is made available under aCC-BY-NC 4.0 International license.




C

| Genomic position (bp) | Gene position (bp) | Protein mutation | Allele frequency in PZQ-ER males | Allele frequency in PZQ-ES males | Effect on channel activation |
|---|---|---|---|---|---|
| 646749 | g.597G>GATA | p.N31ins | 0.6 | 0.06 | None |
| 724853 | g.78701A>ACCG | p.P759ins | 0.80 | 0 | Not tested |
| 724861 | g.78709C>T | p.P757L | 0.76 | 0 | None |
| 724870 | g.78718C>CACT | p.L761ins | 0.77 | 0 | None |
| 724884 | g.78732A>C | p.T765P | 0.70 | 0 | Not tested |
| 724887 | g.78735T>A | p.S766T | 0.79 | 0 | Not tested |
| 741903 | g.95751T>A | p.F992L | 1 | 0 | None |
| 779144 | g.13299G>A | p.R1843Q | 1 | 1 | Not tested |
| 779355 | g.133203A>AC | p.Q1915PfsX2 | 0.99 | 0 | Not tested |
| 779359 | g.133207C>CA | p.G1916RfsX1 | 0.01 | 1 | Not tested |

**Fig. S2. Validation of marker-assisted selection of SmLE-PZQ-ER and ES using Next Generation Sequencing (NGS).** SmLE-PZQ-ER and ES differed only at the locus linked to PZQ resistance (A). Alternatively fixed allele were fixed for alternative alleles at the *Sm.TRPM*$_{PZQ}$-741987C SNP genotyped (B; 1: fixed in ES, -1 fixed in ER), but showed similar allele frequencies across the rest of the genome. Segregating mutations between ER and ES are shown in table (C).

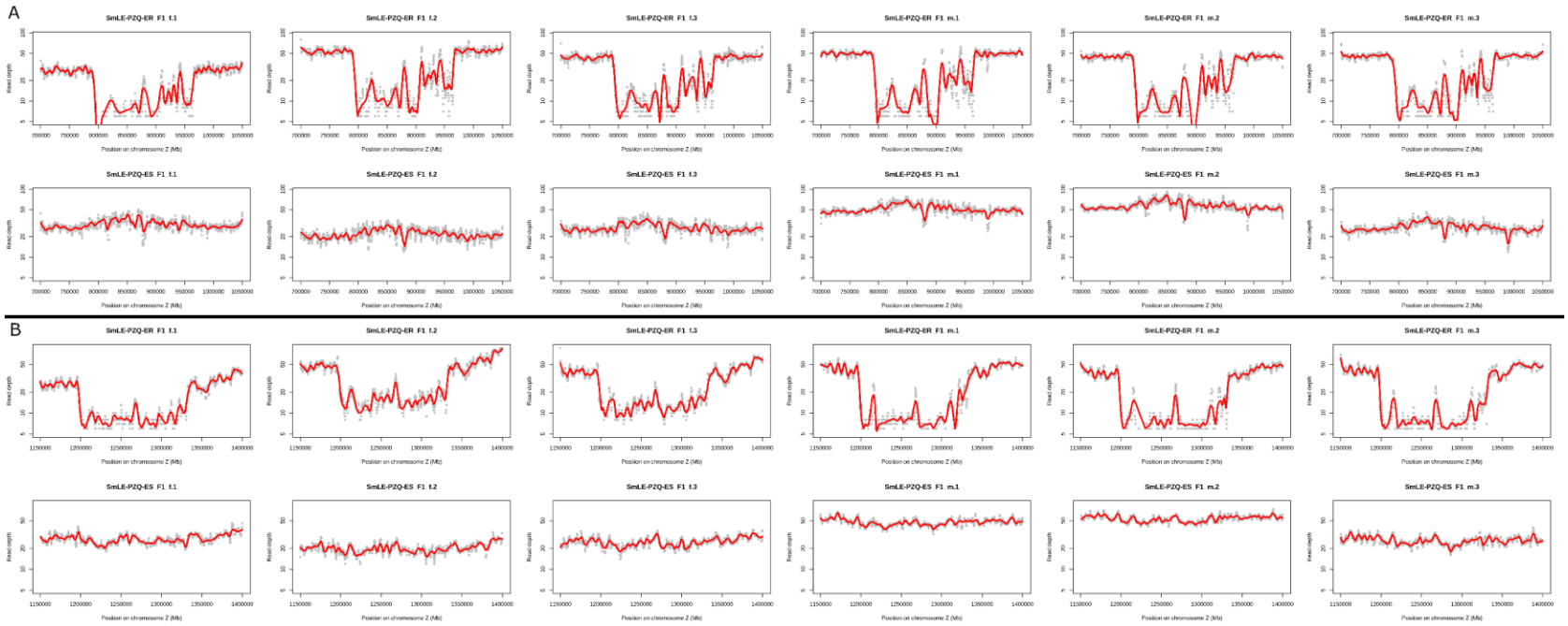



**Fig. S3. Large deletions adjacent to *Sm.TRPM*$_{PZQ}$ and SOX13 transcription factor.** Sequencing of adult parasites recovered from SmLE-PZQ-ER and SmLE-PZQ-ES populations also revealed that the 100 kb (A) and the 150 kb (B) deletions were close to fixation in the SmLE-PZQ-ER population. The first row of each panel refers to the ER population, the second to the ES population. The first three columns refer to the female, the last three columns to the males.

bioRxiv preprint doi: https://doi.org/10.1101/2021.06.09.447779; this version posted June 10, 2021. The copyright holder for this preprint (which was not certified by peer review) is the author/funder, who has granted bioRxiv a license to display the preprint in perpetuity. It is made available under aCC-BY-NC 4.0 International license.



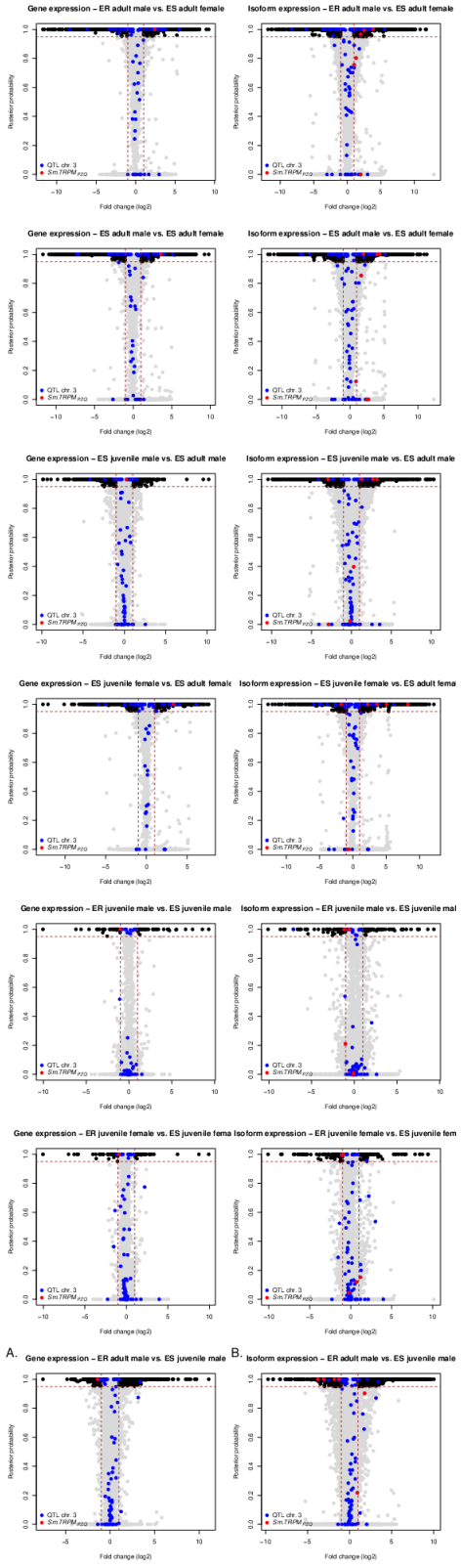



**Fig. S4. Detailed genes and isoforms expression in SmLE-PZQ-ER and SmLE-PZQ-ES parasites.** Comparison of genes and isoforms expression between SmLE-PZQ-ER and ES parasites for each sex (i.e. male and female) and each parasite stage (i.e. adult worm and juvenile worm)

bioRxiv preprint doi: https://doi.org/10.1101/2021.06.09.447779; this version posted June 10, 2021. The copyright holder for this preprint (which was not certified by peer review) is the author/funder, who has granted bioRxiv a license to display the preprint in perpetuity. It is made available under aCC-BY-NC 4.0 International license.

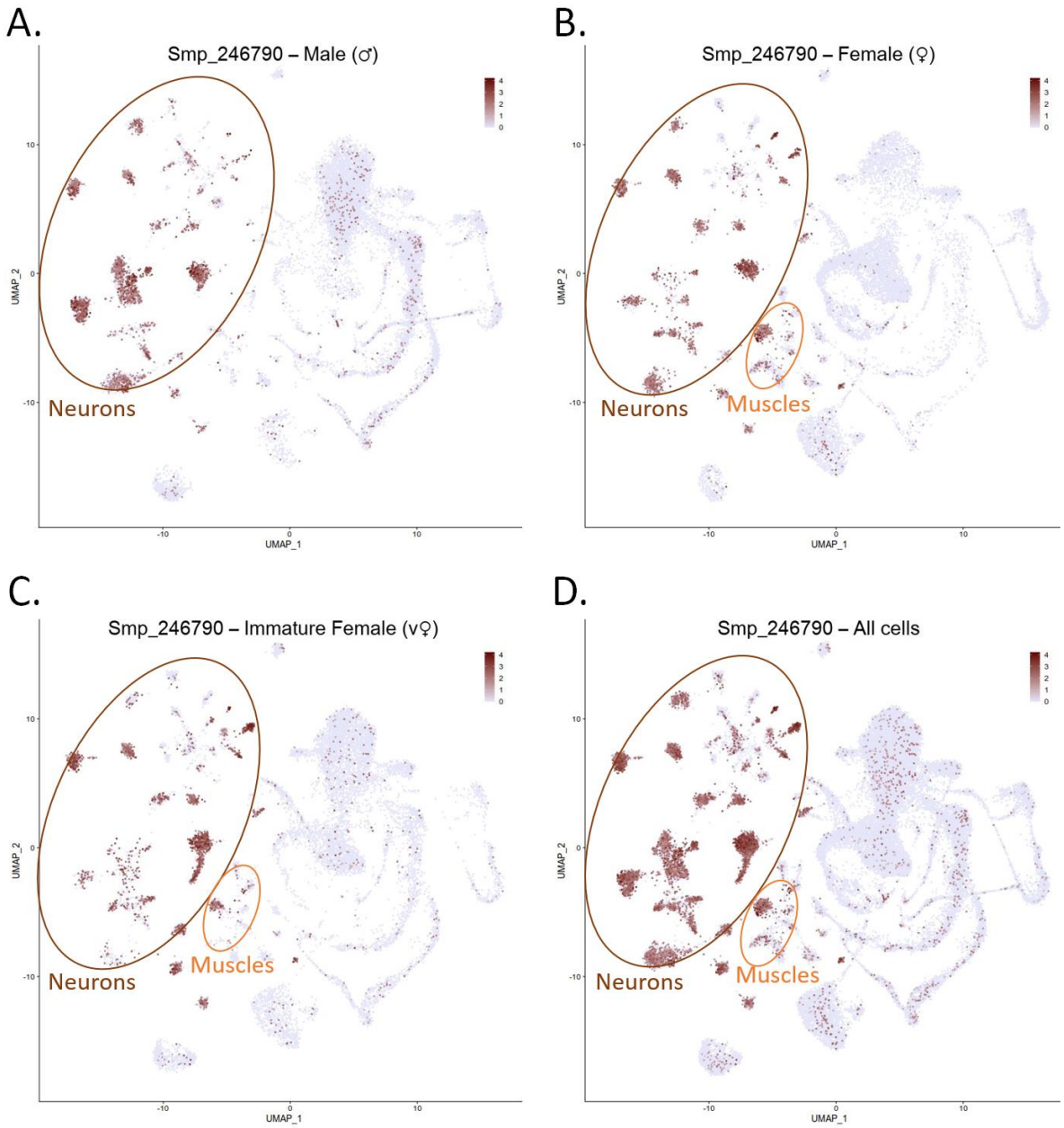



**Fig. S5. Cellular localization of *Sm.TRPM$_{PZQ}$* expression in *S. mansoni*** (A) adult male, (B) adult female, (C) immature female, (D) overall sex and stages (SchistoCyte Atlas *(46)*). *Sm.TRPM$_{PZQ}$* gene is essentially expressed in neurons for all sex and stages and is also expressed in muscle cells in females.

1215

bioRxiv preprint doi: https://doi.org/10.1101/2021.06.09.447779; this version posted June 10, 2021. The copyright holder for this preprint (which was not certified by peer review) is the author/funder, who has granted bioRxiv a license to display the preprint in perpetuity. It is made available under aCC-BY-NC 4.0 International license.



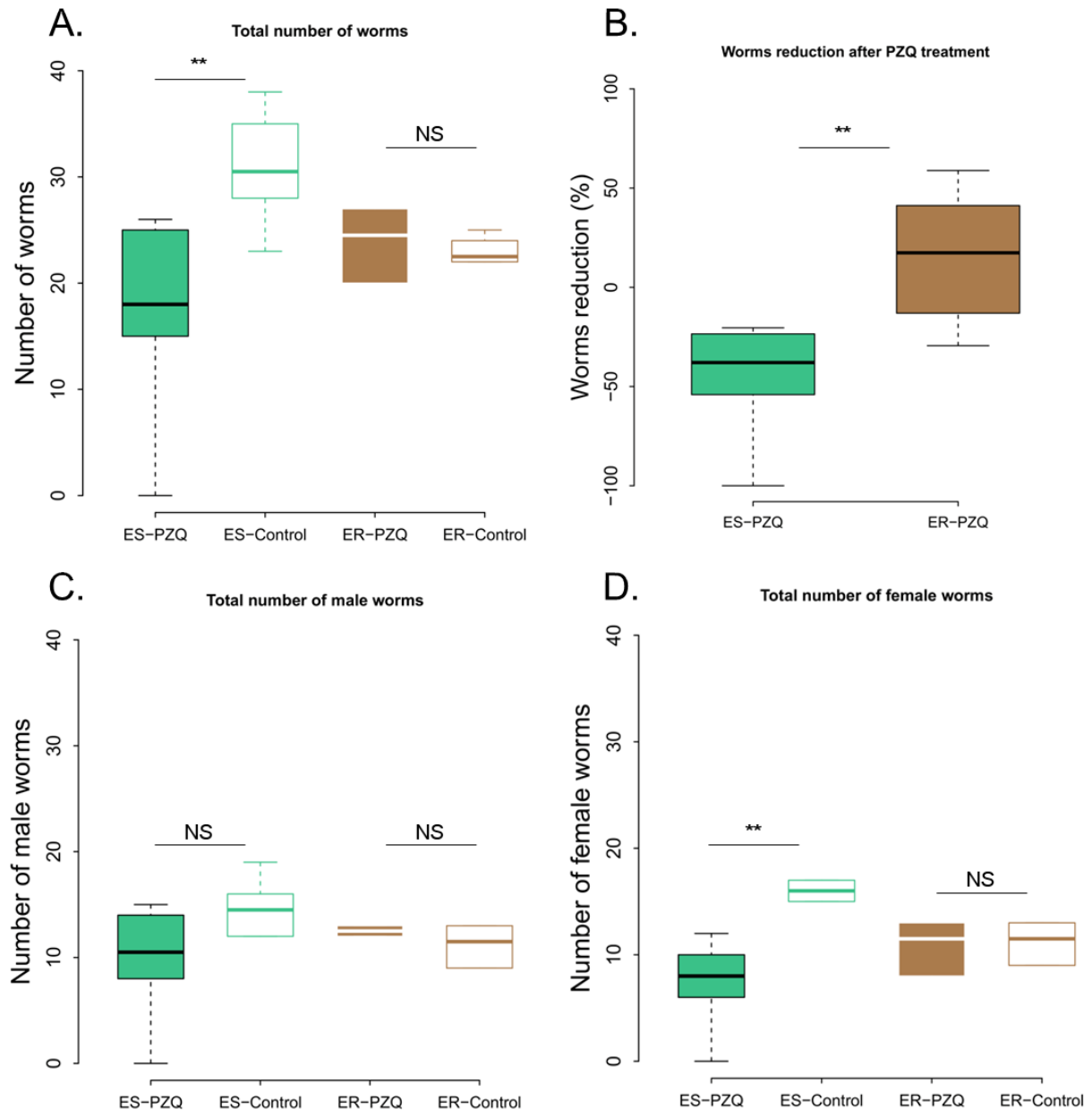



**Fig. S6. Impact of *in vivo* PZQ treatment on SmLE-PZQ-ER and SmLE-PZQ-ES parasites.** Balb/c mice were infected with either SmLE-PZQ-ER or SmLE-PZQ-ES parasites populations and treated with 120 mg/kg of PZQ or DMSO (control group). **(A).** We observed no significant reduction in worm burden in SmLE-PZQ-ER parasites when comparing PZQ-treated and control (DMSO) treated animals (Wilcoxon test, p = 0.393). In contrast, we recovered significantly lower numbers of worms from PZQ-treated versus untreated mice infected with the SmLE-PZQ-ES parasite population (Wilcoxon test, p = 0.008). **(B).** The percent reduction observed was significantly different between the SmLE-PZQ-ES and SmLE-PZQ-ER parasites (Wilcoxon test, p = 0.0129). **(C).** While Interestingly, we did not reach significance for male worms (Wilcoxon test, p = 0.089), **(D).** we observed a large reduction in numbers of female worms recovered from PZQ-treated SmLE-PZQ-ES parasites relative to untreated animals (Wilcoxon test, p = 0.008) ($N$ = 24 mice – 6 mice/group; NS: No significant difference between groups; *$p < 0.05$; ** $p \leq 0.02$; *** $p \leq 0.002$).

bioRxiv preprint doi: https://doi.org/10.1101/2021.06.09.447779; this version posted June 10, 2021. The copyright holder for this preprint (which was not certified by peer review) is the author/funder, who has granted bioRxiv a license to display the preprint in perpetuity. It is made available under aCC-BY-NC 4.0 International license.

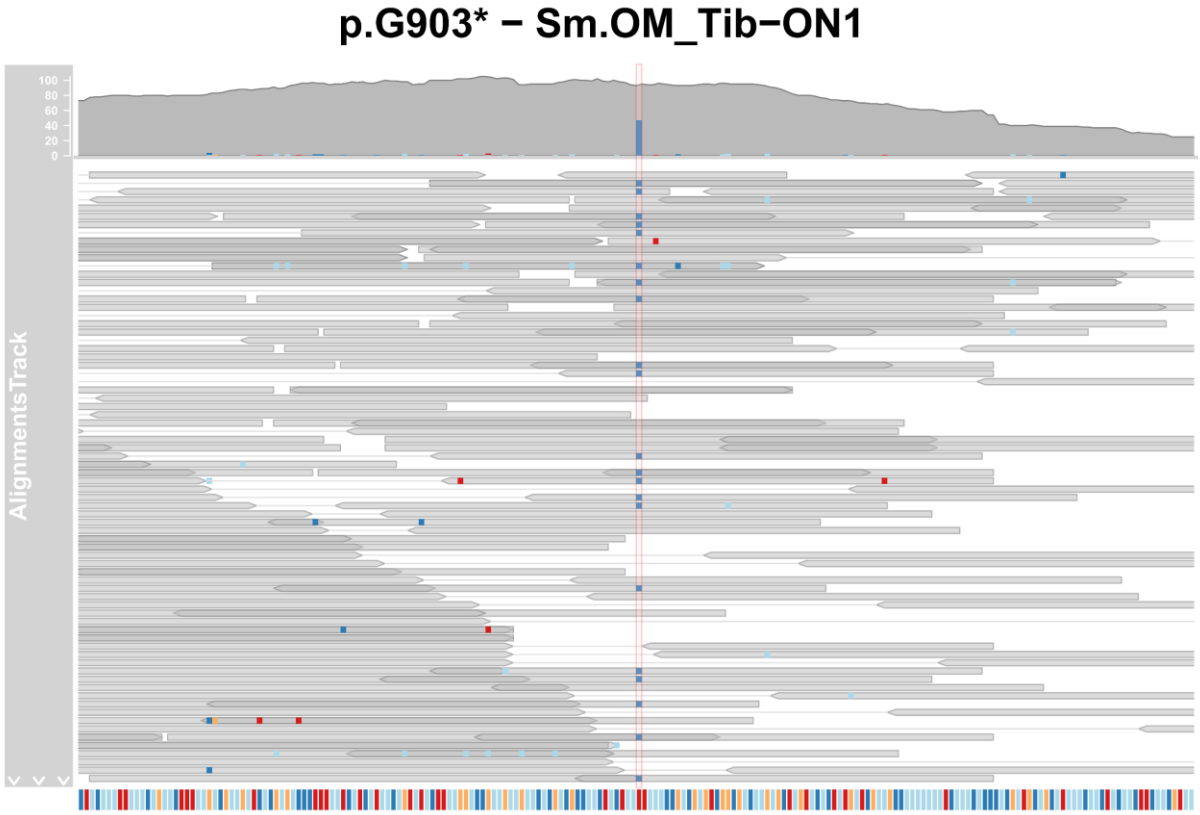



**Fig. S7. Stop codon identified in *S. mansoni* field sample from Oman**. The stop codon p.G903* was identified in NGS exome capture data in one sample collected in Oman. This mutation occurred in exon 14 of the *Sm.TRPM*$_{PZQ}$ gene and the mutation is supported by a high number of reads.

1217

bioRxiv preprint doi: https://doi.org/10.1101/2021.06.09.447779; this version posted June 10, 2021. The copyright holder for this preprint (which was not certified by peer review) is the author/funder, who has granted bioRxiv a license to display the preprint in perpetuity. It is made available under aCC-BY-NC 4.0 International license.

**Table S1. Genes in QTL regions on chr 2 and 3.**

*Separate file*

**Table S2. Summary table of RNAi for Sm.TRPM$_{PZQ}$.** siRNA sequences and primers used to generate dsRNA. Primer sequences used for RT-qPCR to quantify gene expression after RNAi treatment on worms (Chr.: Chromosome; E: Exon). * siRNA negative (scramble siRNA) and positive control (SmAP) have been used from Krautz-Peterson *et al. (79)*.

| Location on the genome | Genomic coordinates | Type | Sequence (5'-3' orientation) | Expected size (bp) | Usage |
|---|---|---|---|---|---|
| Chr. 3 | 646335-646359 | siRNA SmTRP #1 (isoform 5) E1-E2 | AGUACUUUGUUGAAGUCCUUGAATA | - | siRNA |
| Chr. 3 | 724927-724951 | siRNA SmTRP #2 (isoform 5) E10-E20 | CAGCAUUUUUAGAAUGUGAUAAATA | - | siRNA |
| Chr. 3 | 767394-767415 | siRNA SmTRP #3 (isoform 6) E23-E32 | ACCAAGGAGAAUAUGACAUUGAATT | - | siRNA |
| Chr. 4 | 33713410-33713434 | siRNA SmAP* (positive control) | CCACAAGCAUGUUCUCUUACAUACA | - | siRNA |
| - | - | Scrambled siRNA* (negative control) | CUUCCUCUCUUUCUCUCCCUUGUGA | - | siRNA |
| Chr. 3 | 646449-646472 | dsRNA SmTRP #1 (isoform 1-5) – Forward primer | GAAACTGGTACTTTATCCAAGTCC | 614 | dsRNA generation |
| Chr. 3 | 685256-685276 | dsRNA SmTRP #1 (isoform 1-5) – Reverse primer | TCAGCTGCTTTCCATAAACCT | | dsRNA generation |
| Chr. 3 | 700008-700029 | dsRNA SmTRP #2 (isoform 6) – Forward primer | TACAAGTCAACAAAGTGGACCT | 602 | dsRNA generation |
| Chr. 3 | 706699-706721 | dsRNA SmTRP #2 (isoform 6) – Reverse primer | CTTCAATGATGGATTCAAGCCTG | | dsRNA generation |
| - | - | EGFP Forward primer primer with T7 promoter (negative control) | GGTAATACGACTCACTATAGGGAGGTAAACGGCCACAAGTTCAG | 591 | Control RNAi (dsRNA) |
| - | - | EGFP Reverse primer with T7 promoter (negative control) | GGTAATACGACTCACTATAGGGAGGTGCTCAGGTAGTGGTTGTC | | Control RNAi (dsRNA) |
| Chr. 3 | 756865-756887 | SmTRP_qF1– Forward primer | AGTCCTACTTCTGAACAACAAGG | 124 | RT-qPCR |
| Chr. 3 | 757787-757808 | SmTRP_qR1– Reverse primer | TATATTCCACGGTTCTAGCCTG | | RT-qPCR |

| | | | | | |
|---|---|---|---|---|---|
| Chr. 3 | 787906-787927 | SmTRP_qF2 pyrophosphatase domain (isoform 6) – Forward primer | ATCAGCAGTTTGATTACACGTC | 199 | RT-qPCR |
| Chr. 3 | 791384-791407 | SmTRP_qR2 pyrophosphatase domain (isoform 6) – Reverse primer | GAAGTTGAGCTCCTTTACTTTCAG | | RT-qPCR |
| Chr. 4 | 33719124-33719147 | SmAP_qF1 – Forward primer | TCAACTCAGATAGACTCACAACAG | 76 | RT-qPCR |
| Chr. 4 | 33720318-33720338 | SmAP_qR1 – Reverse primer | TTAAATGGCCCTTTCACACCT | | RT-qPCR |
| Chr. 1 | 43164755-43164771 | SmGAPDH_qF2 - Forward primer | CATTGATAAAGCTCAGGCTCAT | 195 | RT-qPCR |
| Chr. 1 | 43164539-43164562 | SmGAPDH_qR2 - Reverse primer | AACTTATCATGAATGACCTTAGCC | | RT-qPCR |

1223

bioRxiv preprint doi: https://doi.org/10.1101/2021.06.09.447779; this version posted June 10, 2021. The copyright holder for this preprint (which was not certified by peer review) is the author/funder, who has granted bioRxiv a license to display the preprint in perpetuity. It is made available under aCC-BY-NC 4.0 International license.

**Table S3. Mutations present in *Sm.TRPM*$_{PZQ}$ in natural schistosome populations from 3 African countries (Senegal, Niger, Tanzania), the Middle East (Oman) and South America (Brazil).**

*Separate file*

1227 **Table S4. Summary table of all the primer sequences** used for i) PCR-RFLP and CNV quantification for single worm genotyping, ii) Sanger

1228 sequencing of Sm.TRPM$_{PZQ}$ in field collected *S. mansoni* parasites (Chr. : Chromosome; E: Exon).

| Location on the genome | Genomic coordinates | Exon coordinate (Gene exon number) | Type | Sequence (5'-3' orientation) | Expected size (bp) | Usage |
|---|---|---|---|---|---|---|
| Chr. 2 | 1071798-1071820 | - | Chr. 2 PCR-RFLP – Forward primer | GACAAGAACCCATCAAGTAACAT | 618 | PCR-RFLP genotyping[a] |
| Chr. 2 | 1072394-1072415 | - | Chr. 2 PCR-RFLP – Reverse primer | GACAAAGCTACCACAACAAACT | | PCR-RFLP genotyping[a] |
| Chr. 3 | 741747-741766 | - | Chr. 3 PCR-RFLP – Forward primer | TCGTAATAAACATGGTCGTC | 421 | PCR-RFLP genotyping[a] |
| Chr. 3 | 742148-742167 | - | Chr. 3 PCR-RFLP – Reverse primer | TCGACTACAGAATGATGTAA | | PCR-RFLP genotyping[a] |
| Chr. 3 | 1220683-1220701 | - | Chr. 3 CNV genotyping – Forward primer | GAAACATTCTGGTCCACCC | 179 | CNV genotyping (qPCR) [b] |
| Chr. 3 | 1220840-1220861 | - | Chr. 3 CNV genotyping – Reverse primer | TGGCTTCAGTATTGAAAGTTGC | | CNV genotyping (qPCR) [b] |
| Chr. 4 | 46055234-46055257 | - | Chr. 4 α-tubulin 2 – Forward primer | CGACTTAGAACCAAATGTTGTAGA | 190 | qPCR (CNV relative quantification) [b] |
| Chr. 4 | 46055405-46055424 | - | Chr. 4 α-tubulin 2 – Reverse primer | GTCCACTACATTGATCCGCT | | qPCR (CNV relative quantification) [b] |
| Chr. 3 | 693769-693788 | 693738-693904 (4) | Sm.TRPM$_{PZQ}$ E 3 – Sanger sequencing – Forward primer | AGGAGTAATGAAGCTAACTG | 140 | Sanger sequencing[c] |
| Chr. 3 | 693891-693909 | 693738-693904 (4) | Sm.TRPM$_{PZQ}$ E 3 – Sanger sequencing – Reverse primer | GTTACCTCATGTAAAGCTG | | Sanger sequencing[c] |
| Chr. 3 | 699775-699792 | 699733-700482 (5) | Sm.TRPM$_{PZQ}$ E 4 – Sanger sequencing – Forward primer | GCTGAAGATAGTGAACCA | 271 | Sanger sequencing[c] |
| Chr. 3 | 700027-700046 | 699733-700482 (5) | Sm.TRPM$_{PZQ}$ E 4 – Sanger sequencing – Reverse primer | TGTGTTGTAGAACTGATAGG | | Sanger sequencing[c] |
| Chr. 3 | 764334-764354 | 764295-764594 (27) | Sm.TRPM$_{PZQ}$ E 23 – Sanger sequencing – Forward primer | GATGGATGGAATAAATTAGAT | 288 | Sanger sequencing[c] |
| Chr. 3 | 764603-764622 | 764295-764594 (27) | Sm.TRPM$_{PZQ}$ E 23 – Sanger sequencing – Reverse primer | CAACATAGAAACAAATCAAA | | Sanger sequencing[c] |

| | | | | | | |
|---|---|---|---|---|---|---|
| Chr. 3 | 771992-772011 | 772107-772214 (29) | Sm.TRPM$_{PZQ}$ E 25 – Sanger sequencing – Forward primer | ATAATGCTTGATTCCCTTCC | 345 | Sanger sequencing[c] |
| Chr. 3 | 772318-772337 | 772107-772214 (29) | Sm.TRPM$_{PZQ}$ E 25 – Sanger sequencing – Reverse primer | TAATCCCACATAGATGACAG | | Sanger sequencing[c] |
| Chr. 3 | 774815-774832 | 774968-775167 (31) | Sm.TRPM$_{PZQ}$ E 27 – Sanger sequencing – Forward primer (1) | CTCCATCAGGAGAAACAG | 418 | Sanger sequencing[c] |
| Chr. 3 | 775214-775233 | 774968-775167 (31) | Sm.TRPM$_{PZQ}$ E 27 – Sanger sequencing – Reverse primer (1) | AAGTATCGTGGCTTATTAGG | | Sanger sequencing[c] |
| Chr. 3 | 774815-774832 | 774968-775167 (31) | Sm.TRPM$_{PZQ}$ E 27 – Sanger sequencing – Forward primer (2) | CTCCATCAGGAGAAACAG | 459 | Sanger sequencing[c] |
| Chr. 3 | 775255-775274 | 774968-775167 (31) | Sm.TRPM$_{PZQ}$ E 27 – Sanger sequencing – Reverse primer (2) | GTACACTTAATTCGTACGAC | | Sanger sequencing[c] |
| Chr. 3 | 778437-778454 | 778446-778595 (33) | Sm.TRPM$_{PZQ}$ E 29 – Sanger sequencing – Forward primer | ATGACTCAGGGTATTGGA | 287 | Sanger sequencing[c] |
| Chr. 3 | 778706-778724 | 778446-778595 (33) | Sm.TRPM$_{PZQ}$ E 29 – Sanger sequencing – Reverse primer | GGGTTGATGGATATTTGGG | | Sanger sequencing[c] |
| Chr. 3 | 787904-787924 | 787852-788001 (38) | Sm.TRPM$_{PZQ}$ E 34 – Sanger sequencing – Forward primer | TTATCAGCAGTTTGATTACAC | 116 | Sanger sequencing[c] |
| Chr. 3 | 788001-788020 | 787852-788001 (38) | Sm.TRPM$_{PZQ}$ E 34 – Sanger sequencing – Reverse primer | CATTATGTTCTATCCATACC | | Sanger sequencing[c] |

[a] PCR condictions for RFLP genotyping: reactions contained 9.325 µL sterile water, 1.5 µL 10x buffer, 1.2 µL dNTP (2.5 mM each), 0.9 µL $MgCl_2$, 0.5µL each primer (10 µM), 0.075 µL *Taq* polymerase (TaKaRa) and 1µL of gDNA template using the following program: 95 °C for 5 minutes, [95 °C for 30s, 55 °C for 30s, and 72 °C for 1min] × 35 cycles, 72 °C for 10 minutes.

[b]qPCR genotpring methods: we conducted qPCR in duplicate for each reaction (samples and standards). Reactions consisted of 5 µL SYBR Green PCR master mix (Applied Biosystems), 3.4 µL sterile water, 0.3 µL of each primer and 1µL of standard PCR product or sample gDNA. We used the following program: 95 °C for 10 minutes, [95 °C for 15s and 60 °C for 1 minute] × 40 cycles followed by a melting curve step (15s at 95 °C and then rising in 0.075 °C increments/second from 60 °C to 95 °C), to check for the uniqueness of the product amplified. We plotted standard curves using seven 10-fold dilutions of a purified i) α-tubulin 2 PCR product (α-tubulin 2 copies. µL−1: $2.21\times10^{2}$ – $2.21\times10^{7}$, efficiency= 87.56%) and ii) CNV region PCR product (Sm.CNV region copies. µL−1: $8.40\times10^{1}$ – $8.40\times10^{6}$, efficiency= 86.17%). PCR products for standard curves were generated as described in LeClech *et al. (80)*. The number of CNV region and α-tubulin 2 copies in each sample was estimated according to the standard curve (QuantStudio Design and Analysis Software). All the primers were designed using PerlPrimer v1.21.1 *(75)*.

[c]PCR conditions for Sanger sequencing: PCRs were performed using the TaKaRa Taq kit (Clontech, USA). For Exon 25 and 27, PCR reactions contained 8.325 µL sterile water, 1.5 µL 10X buffer, 1.2 µL dNTP (2.5 mM each), 0.9 µL $MgCl_2$ (25 mM), 0.5 µL each primer (10 µM), 0.075 µL Taq polymerase (5 U/µL) and 2 µL of DNA template (WGA DNA from *S. mansoni* field collected miracidia from infected patients) (Total reaction volume: 15 µL). For Exon 3, 4, 12, 23, 29 and 34, PCR reactions were done in a total volume of 50 µL (keeping similar volume ratio between the reagents) with 2 µL of DNA template. We used a SimpliAmp Thermal cycler (Applied Biosystems) with the following program: 95 °C for 5 min; 95 °C for 30 s, 53 °C for 45 s, 72 °C for 45 s, for 35 cycles; then 72 °C for 10 min. We verified the presence and size of all PCR products on 2% agarose gels. Ten microliters of PCR products were then cleaned up by adding 4 µL of ExoSAP-IT (Affymetrix USB products) and 2 µL of sterile water and Sanger sequenced in both directions.